HYDRODYNAMIC CHARACTERISATION OF HIGH AND LOW MOLECULAR WEIGHT GLYCANS

RYAN MARK LITHGO, BSc (Hons)

Dissertation submitted to the University of Nottingham for the degree of Master of Research

September 2017

Abstract

Glycans are a diverse group of biological macromolecules that are made up of polysaccharides and glycoconjugates, such as glycoproteins and glycopeptides. The different types of glycans results in a multitude of structures, properties and functions. This investigation looks at the different hydrodynamic properties of several glycans including viscosity, sedimentation coefficient and molecular weight. These parameters are determined using techniques such as viscometry and Analytical Ultracentrifugation (AUC).

A foundation on the principles of the techniques involved in hydrodynamic characterisation was provided through the use of ovalbumin, a glycoprotein that has been extensively studied. The study gave a basic understanding in Analytical Ultracentrifugation.

Using the knowledge obtained from that investigation a study into possible reasons why the 'last-resort' glycopeptide antibiotic, vancomycin, is not commonly administered orally due to poor absorption within the gut. The study examined at the interactions of vancomycin with common macromolecules found with the gastro-intestinal tract, such as mucin, and trying to explain reasons how these interactions could inhibit the absorption of vancomycin.

Finally investigations into two different species derived β-glucans, that have been shown to have medically benefiting properties, were characterised. The used of different hydrodynamic techniques yielded results that generally supported the accepted hydrodynamic properties of β-glucans, however there were results that challenged these understandings as well.

Acknowledgments

I would like to thank my supervisors Professor Stephen Harding and Dr. Gary Adams for guidance and supervision throughout the project, as well as Dr Richard Gillis for his understanding and assistance in analysing the data. I also thank the rest of the NCMH group for their support.

Special thanks go to my family who have supported me in so many ways throughout my degree.

Table of Contents

List of Figures ..... **viii**

List of Tables ..... **xi**

Abbreviations ..... **xiii**

1 Introduction **1**

1.1 Overview 1

1.2 Investigation Aims 4

2 Methods **6**

2.1 Density and Viscosity 6

2.1.1 Density Theory 6

2.1.2 Density Measurements 7

2.1.3 Viscosity Theory 7

2.1.4 Viscosity Measurements 10

2.2 Concentration Determination 11

2.2.1 UV Spectrophotometry 11

2.2.2 Refractometry 12

2.3 Analytical Ultracentrifugation 13

2.3.1 Theory 13

2.3.2 Apparatus 18

3 Hydrodynamic Analysis of an Ovalbumin preparation **20**

3.1 Introduction 20

3.1.1 Aim of Investigation 21

3.2 Materials and Methods 22

3.2.1 Materials 22

3.2.2 Ovalbumin sample preparation and concentration determination 22

3.2.3 Density and Viscosity Measurements 22

3.2.4 Sedimentation Velocity 23

3.2.5 Sedimentation equilibrium 23

3.3 Results and Discussion 24
3.3.1 Concentration measurements 24
3.3.2 Density and Viscometry 26
3.3.3 Sedimentation Velocity 28
3.3.4 Sedimentation Equilibrium 30
3.3.5 Shape Determination 32
3.4 Conclusion 34
4 Evidence of Vancomycin dimerisation and interactions with mucin .35
4.1 Introduction 35
4.2 Materials and Methods 39
4.2.1 Materials 39
4.2.2 Sample Preparations 39
4.2.3 Vancomycin $\bar{v}$ and concentration determination 39
4.2.4 Viscosity Measurements 41
4.2.5 Sedimentation Equilibrium of vancomycin 42
4.2.6 Vancomycin and mucin sample preparation 42
4.2.7 Sedimentation Velocity 43
4.3 Results and Discussion 44
4.3.1 Concentration measurements 44
4.3.2 Viscosity measurements 45
4.3.3 Sedimentation Equilibrium 48
4.3.4 Determining the Association and Dissociation constants 51
4.3.5 Vancomycin and mucin interaction SV analysis 53
4.4 Conclusion 58
5 Hydrodynamic characterisation of β-glucans 59
5.1 Introduction 59
5.1.1 Aim of investigation 61
5.2 Materials and Methods 62
5.2.1 Materials 62

5.2.2 Mushroom (M.P) β-glucan sample preparation 62
5.2.3 Oat β-glucan sample preparation 63
5.2.4 Density and Viscosity measurements 63
5.2.5 Mushroom and Oat β-glucan SV analysis 64
5.2.6 Mushroom and Oat β-glucan SE analysis 65
5.3 Results and Discussion 66
5.3.1 Mushroom β-glucan 66
5.3.2 Oat β-glucan 73
5.4 Conclusion 79
6 Concluding Remarks 80
6.1 Ovalbumin 80
6.2 Vancomycin 81
6.2.1 Future work 81
6.3 Mushroom and oat β-glucan 83
6.3.1 Future work 83
7 References 84

List of Figures

Figure 2.1: Huggins and Kraemer extraction for intrinsic viscosity. Reduced viscosity (●) and inherent viscosity (▲) vs concentration for irradiated (10kGy) guar in phosphate chloride buffer (pH 6.8, I = 0.10). The 'common' intercept gives [η], the slopes K_H $[\eta]^2$ and K_K $[\eta]^2$ (from Jumel, 1994). 8

Figure 2.2: Illustration of Solomon-Ciuta plot. Huggins (black), Kraemer (red) and Solomon-Ciuta (green) extrapolations for λ870 intrinsic viscosity plot (from Jumel, 1994). 10

Figure 2.3: Depictions of Ostwald viscometer. (a) A - the top of the measuring well, B - the bottom of the measuring well, C - U-tube reservoir. (b) Physical depiction of U-tube viscometer (from Poggio et al., 2015) 11

Figure 3.1: Main structural template of the N-linked glycans attached to ovalbumin, (GlcNAc = N-acetylglucosamine). Obtained from Kiely et al. (1976). 20

Figure 3.2: Extrapolation to zero concentration of reduced and inherent viscosities of ovalbumin at 20.0°C. The y-intercept is the intrinsic viscosity value [η]. 27

Figure 3.3: Sedimentation velocity analysis for ovalbumin concentration series. Top: ls-g*(s) analysis. Bottom: c(s) analysis. 28

Figure 3.4: Molar mass analysis for 0.5 mg/mL ovalbumin from SEDFIT-MSTAR: (a) log of concentration in the cell vs the square radial displacment, (b) M* analysis vs radius, (c) point average molecular weight vs local concentration c(r) in the ultracentrifuge cell, (d) point average apparent molecular weight vs radial position in the cell. 30

Figure 3.5: Prolate models of ovalbumin with axial ratios. (A) Shape obtained from Harding (1981) study. (B) Shape determined from results of this investigation. 33

Figure 4.1: Structure of vancomycin with numbered residues, see above. The disaccharide subunit is bound to residue 4 (purple) (Loll et al., 1998). 36

Figure 4.2: Structure of vancomycin with the different atomic environment highlighted. The number of each given atom is also indicated (top right). 40

Figure 4.3: Intrinsic viscosity determination of vancomycin through the extrapolation of the reduced and inherent viscosities to zero concentration, at 20.0°C. 47

Figure 4.4: Changes of weight average molar mass of vancomycin with concentration. M* values (closed signals) and hinge point values (open symbols. Squares: HEPES alone. Circles: HEPES + NaCl. Up triangles: HEPES + NaCl + glycerol. Down triangles: Water + 0.9% NaCl. 49

Figure 4.5: Sedimentation equilibrium plots ($M_{w,app}(r)$ vs c(r)) of each concentration (A-D) overlaid for each solvent condition. (red) 10mg/mL, (orange) 5mg/mL, (green) 2.5 mg/mL, (blue) 1.25 mg/mL and (purple) 0.6 mg/mL. 50

Figure 4.6: Y(c) plots of each solvent conditions at concentrations of 0.60, 1.25 & 2.50 mg/mL: (a) HEPES alone, (b) HEPES + NaCl, (c) HEPES + NaCl + glycerol, and (d) 0.9% NaCl. The slopes of each plot yield the k_2 values. 52

Figure 4.7: Sedimentation velocity ls-g*(*s*) distributions of (Top) 12.5 mg/mL vancomycin and 2.0 mg/mL PGM (x3 repeats) 3000 rpm, (Bottom) 2.0 mg/mL PGM alone 30,000 rpm. 54

Figure 4.8: SV (3000 rpm) distribution of vancomycin + PGM at different concentrations of vancomycin (normalised); 12.5mg/mL (red) (dotted red line, previous study), 1.25 mg/mL (green) and 0.125 mg/mL (blue). 55

Figure 4.9: SV (30,000 rpm) distribution of vancomycin + PGM at different concentrations of vancomycin (normalised); 12.5mg/mL (red), 1.25 mg/mL (green), 0.125 mg/mL (blue) and PGM alone (black). 56

Figure 5.1: Structure of β-glucans derived from mushroom and oat species. (A) Mushroom β,1-3 backbone with β,1-6 branch point, (B) oat β,1-3 and β,1-4 linked backbone. (A) Laroche & Michaud (2007) and (B) Pillai et al. (2005). 60

Figure 5.2: SEDFIT SV analysis of M.P β-glucan concentration series, at a rotor speed of 50,000rpm. (Top) ls-g*(*s*) plot and (Bottom) c(*s*) analysis. 67

Figure 5.3: Molar mass analysis for 0.5mg/mL M.P β-glucan from SEDFIT-MSTAR: (A) Distribution of data along the radius of the cell, (B) log of concentration in the cell vs the square of the radial displacement, (C) M* analysis vs radius, (D) point average molecular weight. 69

Figure 5.4: Prolate models of M.P β-glucans using different hydrations; (A) 0.0, (B) 0.3, (C) 1.0 & (D) 2.0 g water/ g of β-glucan. 72

Figure 5.5: η_{red} (black) and η_{inh} (red) data points of a single concentration of each oat β-glucan sample, with the resulting Solomon-Ciuta (green) values. The data points show the majority of values lie in range of 450 – 1000 mL/g. 75

Figure 5.6: Sedimentation velocity ls-g*(*s*) analysis of all six NOFIMA β-glucan samples (S7-S12), at a rotor speed of 45,000rpm..... 76

Figure 5.7: Molar mass analysis of oat β-glucan Sample 7 (1.5 mg/mL). (A) c(r) vs r, (B) lnc(r) vs r^2, (C) M* vs r & (D) $M_{w,app}(r)$ vs c(r). Hinge point M_w is shown with dotted line..... 77

List of Tables

Table 3.2: Density measurements for varying concentrations of ovalbumin in PBS at 20.0°C 26

Table 3.4: Summary of weight average M_w results for 0.5 and 1.0 mg/mL ovalbumin samples, centrifuged at 20,000rpm 32

Table 4.1: Determination of actual concentration from density measurements for 10.0 & 5.0 mg/mL vancomycin solutions at 20.0°C. 44

Table 4.2: Density measurements at 20.0°C for each nominal dilution with the density correction (ρ/ρ_0) and actual concentration calculated 45

Table 4.3: Average flow times at 20.0°C for each concentration along with the subsequent relative, reduced and inherent viscosities. 46

Table 4.4: Molar mass estimations of vancomycin in the presence of all buffer conditions, showing the M* and hinge point evaluations of M_w. 48

Table 4. 5: k_2, K_2 & K_d values for each buffer concentration. 52

Table 5.1: Relative, reduced, inherent viscosities and intrinsic viscosity of M.P mushroom β-glucans (20.0°C) 66

Table 5.2: Summary of weight averages of M.P β-glucans using M* and hinge point analysis, along with the polydispersity of the samples. 70

Table 5.3: M.P β-glucan concentration comparison between enzyme digestion and refractometry determination (after dialysis). 73

Table 5.4: Reduced and inherent viscosities of all six oat β-glucan samples, along with the Solomon-Ciuta intrinsic viscosity values (Temp= 20.0°C). 74

Table 5.5: The results of all six samples with M* and hinge point molecular weight estimations for all $M_{w,app}$, along with the respective polydispersity indices. Shown also is their respective *s* and Solomon-Ciuta [η] values..... 78

Abbreviations

AUC	Analytical Ultracentrifugation
c(s), g(*s*)	distribution of sedimentation coefficient function
Da, kDa, MDa	Daltons, kilo Daltons, Mega Daltons
dn/dc	refractive index increment (mL/g)
η_r , η_{sp}	relative, specific viscosity
η_{red} , η_{inh} , [η]	reduced, inherent, intrinsic viscosity (mL/g)
k_2	association constant (mL/g)
K_2	molar association constant (mL mol^{-1} or L mol^{-1})
K_D	Dissociation constant (μM)
L	path length (cm)
M	molar concentration (mol/L, mol/mL)
M.P	*Macrolepiota procera*
$M_{w,app}$	apparent weight average molar mass (Daltons, g/mol)
PBS	phosphate buffered saline
PGM	porcine gastric mucin
ρ , ρ_0	solution , solvent density (g/mL)
rpm	revolutions per minute
s	sedimentation coefficient (seconds, s / Svedbergs, S)
$s_{20,w}$	sedimentation coefficient, corrected to solvent conditions (viscosity and density of water at 20°C) Sedimentation coefficient corrected for non-ideality
S	Svedberg unit = 1 x 10^{-13} s
$\bar{v}$	partial specific volume (mL/g)

1 Introduction

1.1 Overview

Glycans are a diverse and complex group of biological macromolecules, composed of polysaccharides, oligosaccharides and glycoconjugates such as glycoproteins (Harding et al., 2017). The work presented throughout this MRes shows the hydrodynamic characterisation of four different types of glycans. 1) ovalbumin (glycoprotein), 2) vancomycin (glycopeptide) and 3) two β-glucans (polysaccharides) derived from oat and mushroom species. The aim of the study is to determine their intrinsic properties such as viscosity, molecular weight and sedimentation coefficients using hydrodynamic techniques.

This study is concerned with the hydrodynamic characterisation of macromolecular glycans, where hydrodynamics can be defined as the study of a macromolecule's movement through or with a solvent, which may be water or another aqueous medium (e.g. buffer solution). Although low in resolution compared to other techniques such as crystallography, hydrodynamics yields information regarding the general shape, structure and molecular weight of macromolecules in what for many is their natural environment (Harding, 1995). In order to look at the hydrodynamic properties of different macromolecular glycans several methods will be adopted for this investigation. The main methods adopted include viscometry, density measurement and Analytical Ultracentrifugation (AUC) as well as other methods.
The main characterising instrument used in this investigation was AUC, consisting of two methods: sedimentation velocity (SV) and sedimentation equilibrium (SE).

Sedimentation velocity is a method whereby a high rotor speed is applied in order to sediment any macromolecules present within a given system. Optical systems within the AUC track the rate of sedimentation (concentrations as a function of radius and time). The sedimentation data was analysed using the powerful algorithm SEDFIT(15b) which provides a platform for the analysis of sedimentation data against the Lamm equation (Lamm, 1929). The result of this analysis is that the distribution data is fitted to the best model that resolves the equation, this allows the sedimentation coefficient distribution and weight average sedimentation coefficient, *s*, for the given macromolecule to be obtained (Schuck, 2000). The

sedimentation coefficient can then be used to estimate the shapes of regular shaped macromolecules (such as globular proteins), using for example the ELLIPS suite of modelling algorithms (Harding et al., 1997b), or for more complex macromolecules the HYDRO suite of bead modelling algorithms (Garcia de la Torre & Harding, 2013). For flexible linear structures the HYDFIT set of algorithms are useful (Ortega & Garcia de la Torre, 2007)

Sedimentation equilibrium (SE) is a method which involves the use of lower rotor speeds in order to reach an equilibrium point whereby the rate of sedimentation is matched by diffusion of the macromolecules. The lack of a net force in either direction results in no net movement of the distribution of macromolecules within the cell. The stationary state removes factors friction dependent factors including the shape of the macromolecule and is only dependant on the molar mass of the macromolecule (see, for example, Cole et al., 2008). The data obtained from the AUC is analysed using SEDFIT-MSTARv.1 which is an implementation of the MSTAR algorithm (Creeth & Harding, 1982) on the SEDFIT(15.b) platform and provides the weight average molar mass of the macromolecules (Schuck et al., 2014).

In addition to AUC, other methods applied in this investigation include viscosity and density measurements, both of these hydrodynamic parameters are used within AUC analysis.

The work in this dissertation investigates the hydrodynamic characterisation of three different glycans.
Glycoproteins are a common glycoconjugate macromolecule found in nature. They are protein molecules with polysaccharides attached to the amino acid backbone. The attachment of polysaccharides to the protein occur during or post translation, and are sometimes required for the correct folding of the protein (Spiro, 2002).

Ovalbumin is a glycoprotein that is the main constituent protein found in egg whites, it has a molecular weight of approximately 45,000 Daltons, of which the glycans make up approximately 4% by weight. The attachment of the glycans are made using N-linked glycosidic bonds to mainly asparagine residues on the ovalbumin molecule (An et al., 2003). Ovalbumin is a member of the serine proteinase inhibitor (SERPIN) family which includes enzymes such as antitrypsin (Carrell et al., 1985). Although a member of the SERPIN superfamily ovalbumin does not show any inhibitory activity towards serine proteases, this suggests that

its function is still not fully understood (Huntington et al., 2001). The lack of understanding in the function of ovalbumin is compensated by the well-defined structure and hydrodynamic properties of the protein macromolecule (Nisbet et al., 1981). Chapter 3 looks at obtaining a general understanding of different hydrodynamic analysis techniques through the characterisation of a preparation of ovalbumin. The investigation will determine some of the hydrodynamic properties of ovalbumin such as viscosity, density and sedimentation coefficients, using process including viscometry and analytical ultracentrifugation amongst other.

Another related class of glycans are the glycopeptides. These are similar to glycoproteins however they are formed from only a few amino acids to which are attached oligosaccharides or in some cases polysaccharides (Hojo et al., 2007). Glycopeptides are used for a number of applications within nature, one of which is as antibiotics. The antibiotic properties of certain glycopeptides are of interest, especially with the emergence of antibiotic resistance within bacteria (Hiramatsu, 2001). One such antibiotic glycopeptide of interest at the moment is vancomycin, this is a 'last resort' antibiotic used against gram-positive bacteria such as *Staphylococcus aureus* (MRSA) (Small et al., 1990). Vancomycin is a small glycopeptide with a molecular weight of 1449 Daltons, it is composed of several modified amino acids and a disaccharide of vancosamine-glucose (Jia et al., 2013). Vancomycin works through binding to the D-alanyl-D-alanine residues of peptidoglycan found in the gram-positive bacteria's cell walls. The binding to the peptidoglycan inhibits cell wall growth and eventually leads to lysis of the bacteria cell. The binding of dimeric vancomycin to these residues has long been known, this investigation however looks at the characterisation of dimeric vancomycin in the absence of their ligand.

The preferred administration method of vancomycin for patients is intravenously. Oral administration of vancomycin is less preferred as vancomycin is poorly absorbed within the intestine so has to be taken more frequently. This poor absorption has been known for a long time and common practice is to administer 3 or 4 doses daily, if oral administration is necessary, however oral vancomycin often results in indigestion (Lucas et al., 1987 & Fekety et al., 1989). The reasons why vancomycin is poorly absorbed by the intestine are not fully understood. This study also investigates if vancomycin interacts with gastric mucin, a large glycoprotein and main component of the gastrointestinal tract (Kararli, 1995). The investigation will evaluate if any interaction with mucin could contribute to the poor absorption of vancomycin.

Chapter 5 involves the investigation of a class of the most common glycans found within nature, polysaccharides. These are long chain polymers composed of monosaccharide subunits. Polysaccharides normally have high molecular weights, high polydispersity and generally have less defined shapes and structures compared to proteins (Harding et al., 2017). The investigation involves a specific class of polysaccharide, β-glucan, derived from oat and wild mushroom species. These macromolecular glycans are of interest not only in foods but also in the field of health sciences as they have been shown, especially oat derived β-glucans, to aide in reducing cholesterol levels within the body (Ho et al., 2016).

The basic structure of β-glucans are the same in all species. They are long chain polymers composed of D-glucose monomers. Although the monosaccharide subunits are the same between species, the glycosidic bonds that link them differ between species. Fungal β-glucans are often short chained polysaccharides linked through β,1-3-glycosidic bonds with β,1-6 branching, they tend to be low in molecular weight (Han et al., (2008) & Wasser, (2002)). Oat β-glucans tend to have high molecular weights resulting in them being structurally larger. In comparison to mushroom β-glucans, they form β,1-3 and β-1,4 glycosidic bonds (Brennan et al., 2005). The different glycosidic linkages found within the β-glucans result in different shapes and structures being adopted by both types. The differences in shape, combined with the different molecular weights, give varying hydrodynamic properties such as viscosity and sedimentation coefficients for each species. The determination of the each β-glucans hydrodynamic properties are explored in Chapter 5 and compared.

1.2 Investigation Aims

The overall aim of this investigation is to use different hydrodynamic analysis methods to characterise several different types of glycans using methods including AUC and viscosity.

- The aim of Chapter 3 is to understand how hydrodynamics and in particular AUC can assay for the purity/heterogeneity of a preparation of a glycoprotein - ovalbumin - with a low degree of glycosylation.
- Chapter 4 aims to utilise and build on the hydrodynamic methods used in Chapter 3 to analyse the glycopeptide vancomycin. The investigations aims

to characterise the dimerisation of vancomycin and obtain a dissociation constant, as well as investigate the possible interaction with mucin.

- Chapter 5 looks at the differences in the hydrodynamic properties of polysaccharides (i.e. glycans with 100% glycosylation) namely the relatively low molecular weight mushroom β-glucans and the relatively high molecular weight oat β-glucans. The investigation uses viscometry and AUC to determine viscosity, molecular weight and conformation.

2 Methods

2.1 Density and Viscosity

2.1.1 Density Theory

Solution density measurements can be used in order to find several different parameters of a given macromolecule, including amongst others, the partial specific volume ($\bar{v}$) and the concentration of a sample. By measuring density we can also convert kinematic viscosities into dynamic (density corrected) viscosities (see Harding, 1997)

The density of a macromolecular solution can affect its behaviour in a solution, such as viscosity behaviour as shown in equation (2.3).

The density of a macromolecular solution can be used to find its partial specific volume. This is the reciprocal of the anhydrous density of the macromolecule. Proteins and polysaccharides have a $\bar{v}$ value approximately 0.73 and 0.60 mL/g respectively (Hunter, 1966). In general polysaccharides are more dense than proteins therefore resulting in a lower partial specific volume. Equation (2.1) shows the relationship between density and partial specific volume (Kratky et al., 1973).

$$\bar{v} = \frac{1}{\rho_0} \times \left(1 - \frac{\rho - \rho_0}{c}\right) \qquad (2.1)$$

Where (ρ) is the density of the macromolecular solution, (ρ_0) is the solvent density and c is the concentration of the sample (g/mL). Rearranging Equation (2.1) enable the concentration of a solution to calculate if the $\bar{v}$ is known.

$$c = \frac{\rho - \rho_0}{1 - \bar{v}\,\rho_0} \qquad (2.2)$$

2.1.2 Density Measurements

Density measurements were made using an Anton Paar DMA5000 oscillating capillary meter. Samples were purged after entry into the density meter (approximately 2mL) ensuring no air bubbles were present within the capillary. The samples were left to equilibrate to 20.00°C whereupon the density measurements were recorded to seven significant figures.

2.1.3 Viscosity Theory

Viscosity is a measure of a solutions resistance to flow, such that a more viscous material (e.g. honey) flows more slowly than a less viscous material (e.g. water). The intrinsic viscosity [η] relates to the viscosity of a macromolecule in solution. It is a measure of the shape and size of the macromolecule and is derived through the flow times of solutions using the relative viscosity (η_r):

$$\eta_r = \frac{\eta}{\eta_0} = \left(\frac{t}{t_0} \times \frac{\rho}{\rho_0}\right) \tag{2.3}$$

where η and η_0 are the dynamic viscosity of the solution and solvent, t and t_0 are the flowtimes of the solution and solvent and ρ and ρ_0 are the solution and solvent densities respectively. The density correction is important for solution concentrations >5mg/mLs.

From the relative viscosity the reduced viscosity (η_{red}) can be determined using the concentration of the solution (**c**):

$$\eta_{red} = \frac{(\eta_r - 1)}{c} \tag{2.4}$$

In conjunction with the reduced viscosity, the inherent viscosity (η_{inh}) is another method for determining the intrinsic viscosity using the natural logarithm of the relative viscosity:

$$\eta_{inh} = \frac{\ln(\eta_r)}{c} \tag{2.5}$$

Both the reduced and inherent viscosities are dependent on concentration as a result of non-ideality. This can occur through different mechanisms including charge interaction and size exclusion. In order to eliminate the effect of non-ideality the reduced and inherent viscosity are plotted against concentration, with extrapolations of both data sets to zero concentration. Upon approaching zero concentration non-ideality is reduced to almost zero as the possible interactions between macromolecules are reduced as to almost be negligible. Therefore the value of the reduced and inherent viscosities at zero concentration is termed as the intrinsic viscosity [η].

Both the reduced and inherent viscosities extrapolated to ideal conditions (c=0) should produce the same intrinsic viscosity value, Figure 2.1 illustrates this.

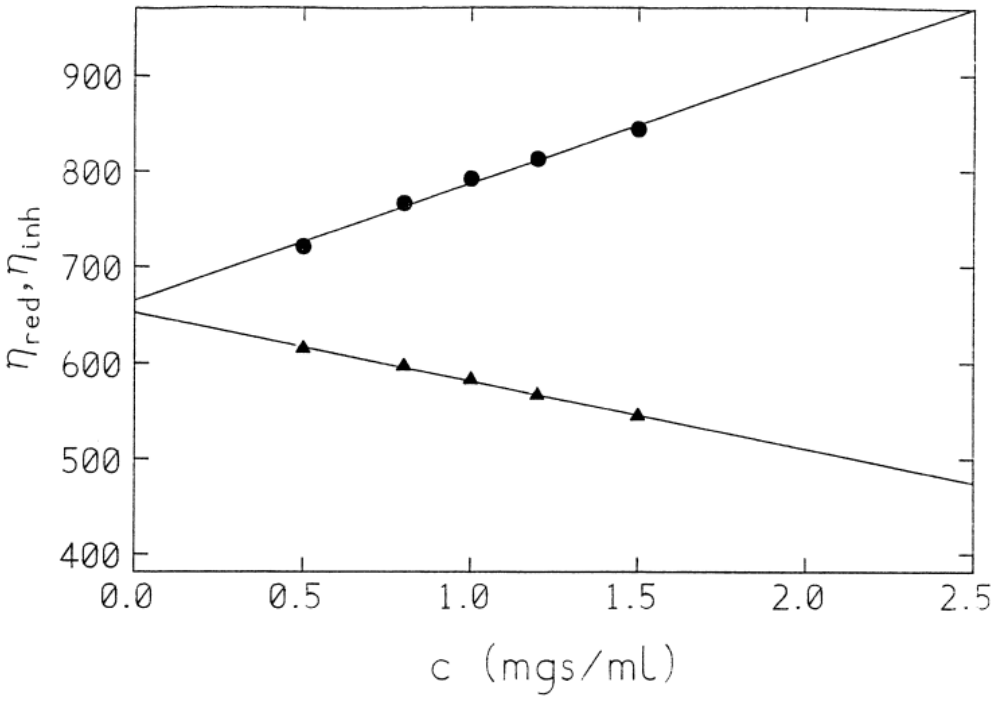

Figure 2.1: Huggins and Kraemer extraction for intrinsic viscosity. Reduced viscosity (•) and inherent viscosity (▲) vs concentration for irradiated (10kGy) guar in phosphate chloride buffer (pH 6.8, *I* = 0.10). The 'common' intercept gives [η], the slopes K_H $[\eta]^2$ and K_K $[\eta]^2$ (from Jumel, 1994).

$$\lim_{c\to 0}(\eta_{red}) = \lim_{c\to 0}(\eta_{inh}) = [\eta] \qquad (2.6)$$

From the plot of the reduced and inherent viscosities, Figure 2.1, two parameters can be determined the Huggins and Kraemer constants K_H and K_K respectively (Sakai, 1968). Equations (2.7 & 2.8) show the relationship between the reduced viscosity and Huggins constant and between the inherent viscosity and the Kraemer constant, respectively (see Harding, 1997).

$$\eta_{red} = [\eta](1 + [\eta].K_H.c) \quad , \quad K_H = \left(\frac{slope}{[\eta^2]}\right) \qquad (2.7)$$

$$\eta_{inh} = [\eta](1 - [\eta].K_K.c) \quad , \quad K_K = -\left(\frac{slope}{[\eta^2]}\right) \qquad (2.8)$$

A combination of the Huggins and Kraemer equations is the Solomon-Ciuta equation (2.9).

$$[\eta] = \left(\frac{1}{c}\right) \times [\, 2(\eta_r - 1) - 2\ln(\eta_r)]^{\frac{1}{2}} \qquad (2.9)$$

which allows an approximate estimation of [η] if only a single concentration has been measured. When plotted against concentration as in Figure 2.1, a linear line that lies between the reduced and inherent viscosity extrapolations occurs. Figure 2.2 illustrate this.

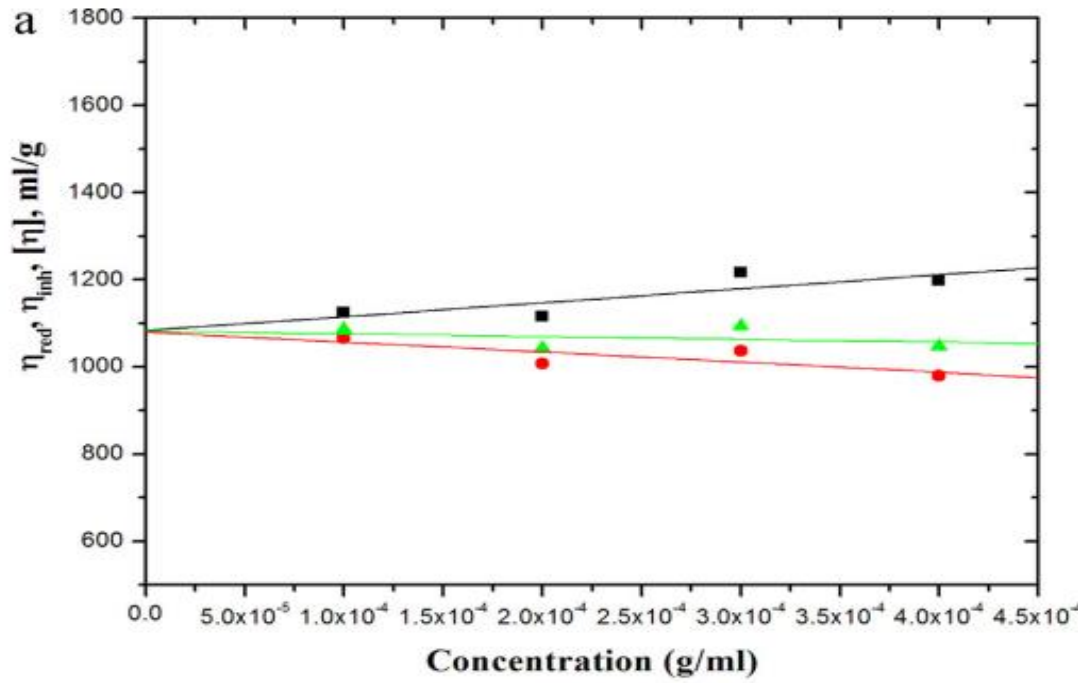

Figure 2.2: Illustration of Solomon-Ciuta plot. Huggins (black), Kraemer (red) and Solomon-Ciuta (green) extrapolations for λ870 intrinsic viscosity plot (from Jumel, 1994).

2.1.4 Viscosity Measurements

As stated in 2.1.3 the flow times of macromolecular solutions need to be measured in order to determine the intrinsic viscosity through parameters such as the relative viscosity (see, Harding, 1997).

To accurately measure the flow times of the samples they were placed into a glass Ostwald U-tube viscometer (Figure 2.3). A number of variables can affect the viscosity of a solution the biggest being temperature, therefore in order to eliminate this possibility the U-tube was placed into a water bath regulated by a Grant GD120 heater pump at (20.00$\pm$ 0.05)°C. The samples were then injected into the reservoir of the U-tube (approximately 2mL) and left to adjust to the water bath temperature.

In order to measure the flow times the U-tube was connected to a Schott-Geräte AVS 400 pump and timing unit. The samples were pumped through the capillary of the U-tube to the top of the measuring well. The samples were then allowed to flow back through the capillary under the force of gravity alone. The time taken

for the meniscus to move from the top of the well to the bottom was recorded by the optics of the AVS 400 (refer to Figure 2.3 (a)).

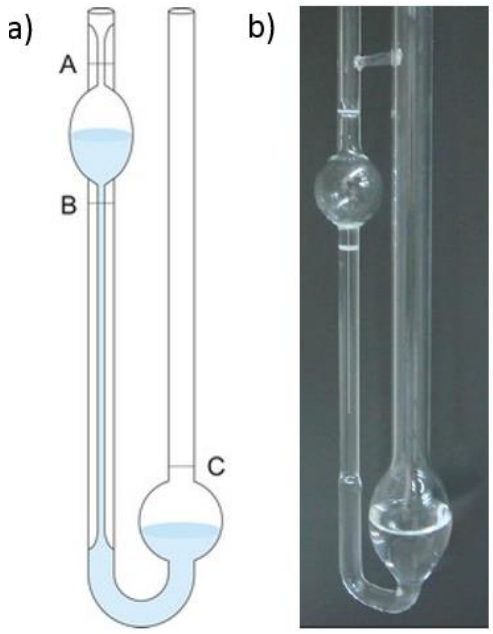

Figure 2.3: Depictions of Ostwald viscometer. (a) A the top of the measuring well, B the bottom of the measuring well, C U-tube reservoir. (b) Physical depiction of U-tube viscometer (from Poggio et al., 2015)

Using the flow times, and subsequent corresponding density measurements, the relative viscosity can be determined through Equation (2.1).

2.2 Concentration Determination

2.2.1 UV Spectrophotometry

Concentration is critical in determining many parameters of a macromolecule, therefore it is essential to accurately measure this parameter. UV spectrophotometry is a method which determines the concentration of a solution through the Beer-Lambert law, Equation (2.10);

$$A = \boldsymbol{\varepsilon}_{280nm} \,.\, L \,.\, c \qquad , \qquad c = \frac{A}{\boldsymbol{\varepsilon}_{280nm} \,.\, L} \tag{2.10}$$

Where A is the absorbance of the solution, $\boldsymbol{\varepsilon}_{280nm}$ is the extinction coefficient of the macromolecule at 280nm (L mol^{-1} cm^{-1}), *L* is the path length (cm) and c is the concentration of the solution (g/mL).

The Beer-Lambert law is useful for determining the concentration of macromolecule solutions which have a chromophore within their structure. Chromophores absorb UV light, it is the absorption (change in light intensity) of the UV light that the spectrophotometer detects. The change in light intensity is directly proportional to the concentration of the solution.
Although the Beer-Lambert law can be applied to macromolecules such as proteins, it is not possible to use this technique on polysaccharides as they do not contain a chromophore within their structure.

Measurements of the UV absorption were performed using a Varian Cary-50 Probe UV-Vis Spectrophotometer. Samples were placed into a 1mL reduced volume quartz cuvette and placed into the spectrophotometer. Measurements were made using a wavelength of 280nm. This was chosen as the chromophores in proteins are aromatic groups found on phenylalanine, tryptophan and tyrosine amino acids and absorb UV light at this wavelength.

2.2.2 Refractometry

Refractometry is another method which can measure the concentration of a macromolecule solution by using a refractometer. This method can be applied to most macromolecule solutions as it does not rely on the presence of chromophores. For this purpose it is the predominant method for determining the concentration of polysaccharide solutions.

Refractometry works on the principle that all macromolecular solutions bend the direction light at different amounts. For a given wavelength this depends in the concentration and the refractive index (dn/dc). The bending of light is affected by the refractive index of the molecule as well as the concentration of the solution, the higher the concentration the greater the bending of the light. Using this principle the concentration of a solution can be made using Equation (2.11).

$$\text{Concentration} = \text{Brix}(\%) \times \left(\frac{\left(\frac{dn}{dc}\right)\text{molecule}}{0.15} \right) \times 10 \text{ (mg/mL)} \qquad (2.11)$$

Where Brix (%) is the percentage measure and 0.15 is the dn/dc of sucrose in mL/g (used as a standard).

Measurements were made using an ATAGO DD-7 differential refractometer. The apparatus was zeroed by purging approximately 3mL of the solvent through the refractometer. Once blanked, solution measurements were made in the same way, Brix (%) were recorded for each measurement.

2.3 Analytical Ultracentrifugation

Analytical Ultracentrifugation (AUC) is a quantitative technique for measuring solutions of macromolecules. AUC works on the principle that under a centrifugal force, molecules with different molecular weights and shapes separate and sediment through a solvent at different rates. The rate of sedimentation is largely affected by the mass of the macromolecule. The greater the molar mass the faster the molecule sediments (Svedberg et al., 1926). As explained in Chapter 2 there are 2 types of AUC measurements; sedimentation velocity (SV) and sedimentation equilibrium (SE). Each method provides different information of the hydrodynamic properties of the macromolecule being analysed.

2.3.1 Theory

2.3.1.1 Sedimentation Velocity (SV)

Herein lies a summary of the method taken from (Ralston, 1993) Sedimentation velocity involves the application of a large centrifugal force to a macromolecular solution over a period of 12 -18 hours. The force is applied through spinning the solution at a high rotor speed and the sedimentation is tracked using absorbance or Rayleigh interference optics.

The high rotor speeds allow the macromolecules to sediment. The rate of sedimentation, divided by the force applied, is termed the sedimentation coefficient (*s*) of the macromolecule. Sedimentation coefficients are dependent upon the size and shape of the macromolecule. Generally, the larger the macromolecule the faster it sediments thus a larger sedimentation coefficient (Svedberg et al, 1926). The Svedberg equation in Equation 2.12 shows the relationship between molar mass and sedimentation coefficient.

$$s = \frac{v}{\omega^2 r} = \frac{M(1- \bar{v}\,\rho_0)}{N_A f} \qquad (2.12)$$

where (s) is the sedimentation coefficient, (v) is the boundary terminal velocity, (ω) is the angular velocity (radians/second), (r) is the radius from the centre of rotation, (M) is the molar mass,($\bar{v}$)is the partial specific volume, (ρ_0) is the solvent density, (N_A) is Avogadro's number and (f) is the frictional coefficient.

In monodisperse solutions the rate of sedimentation should be uniform as the macromolecules are the same molecular weight. However polydispersed systems often show a non-uniform sedimentation profile. This is due to the macromolecules having different molecular weights and shapes that result in different sedimentation rates.

In addition to the effects of mono and polydispersity the effects of the solvent on the sedimentation of the macromolecules have to be taken into account. The solvent will have its own viscosity and density which will affect the sedimentation rate of the macromolecule. Therefore in order to overcome this the sedimentation coefficient is often corrected to standard solvent conditions, namely the viscosity and density of water at 20.0°C. Equation (2.13) shows the correction equation, where the subscripts ($_{20,w}$) denotes the corrected values and (T,b) are the experimental values obtained.

$$s_{20,w} = \frac{(1- \bar{v}\rho)_{20,w}}{(1- \bar{v}\rho)_{T,B}} \times \frac{\eta_{T,B}}{\eta_{20,w}} \times s_{T,b} \qquad (2.13)$$

Sedimentation velocity data was analysed using the computer programme SEDFIT (Schuck, 2000). This aims to fit a model to the data to a 'best fit' that yields the most accurate sedimentation coefficient. In order to model the data SEDFIT uses two algorithms; the least square Gaussian distribution (ls-g*(s)) and continuous distribution (c(s)). The two algorithms are based upon the Lamm equation (2.14) (Lamm, 1929). The equation is used to fit the data to the best solution to the equation which describes the shape of the boundaries formed through sedimentation.

$$\frac{dc}{dt} = D\left[\left(\frac{d^2c}{dr^2}\right) + \frac{1}{r}.\left(\frac{dc}{dr}\right)\right] - s\omega^2.\left[r\left(\frac{dc}{dr}\right) + 2c\right] \qquad (2.14)$$

Equation (2.14); D is the diffusion coefficient, c is the concentration, r is the radial position and t is the time.

In order to determine the best model for the data, using either ls-g*(*s*) or c(*s*) analysis, SEDFIT removes time invariant (TI) and radial invariant (RI) noise. The removal of this noise increases the resolution of the data and represents the data more accurately (Schuck et al., 1999).

The least square Gaussian distribution algorithm analyses the raw SV data against a number of parameters and models it against *s*. The modelling of the data does not take into account the diffusion of the macromolecules within the solution, this means that the model is not fully representative of what is happening during sedimentation within the cell. The result of diffusion not being taken into account results in the broad peaks on the plot, however even though the peaks are relatively broad they give a good indication of the sedimentation coefficient.

The so-called c(*s*) analysis uses a similar algorithm however it takes into account diffusion. The impact of diffusion on very large macromolecules is small and in some cases negligible. The greater impact comes when smaller macromolecules are in solution (Schuck, 2000). The diffusion coefficient is determined by finding the frictional ratio of the macromolecule. The frictional ratio is the frictional coefficient of the observed macromolecule to that of a perfect sphere of the same molecular weight (Brown et al., 2006). With the addition of diffusion within the algorithm more defined peaks are often observed within the c(*s*) distribution. This has benefits in providing more accurate sedimentation coefficients, however it can also lead to over-sharpening of some peaks that may not be accurate (Schuck, 2000). The addition of diffusion within the calculation also results in c(*s*) distributions being able to estimate the weight average molar mass by transforming c(*s*) distributions into c(M) vs M plots. This is applicable for systems of low polydispersity (e.g. mixtures of proteins) and where the components have similar diffusion coefficients. Continuous distributions we use a different programme call the *Extended Fujita* method (Harding et al., 2011).

Sedimentation velocity analysis for monodispersed systems, such as proteins, yield sharper more defined peaks as there is only one macromolecule species in solution, allowing a higher degree of accuracy in the estimation of the sedimentation coefficient. However polydispersed systems, such as polysaccharides, or heterogeneous preparations of a protein or glycoprotein, produce more broad peaks with a lower degree of sharpness as there are multiple macromolecules with different molecular weights. This results in an average sedimentation coefficient being obtained. In addition the areas under the curves for both g(*s*) and c(*s*) are related to the concentration of the macromolecules within the cell.

In order to obtain more accurate sedimentation coefficients concentration series are prepared, this is to reduce non-ideality factors affecting the sedimentation rate. The results are plotted as *s* (or 1/*s*) vs concentration with an extrapolation to zero concentration as to obtain the actual sedimentation coefficient independent of concentration.

2.3.1.2 Sedimentation Equilibrium (SE)

Sedimentation equilibrium experiments involve solutions of macromolecules being centrifuged at lower speeds than in SV runs. The balance between sedimentation and diffusion, results in no overall net movement of the macromolecules within the cell (for example Cole et al., 2008; Schuck et al., 2014). The choice of speed for equilibrium runs is of paramount importance. Too high or too low and the macromolecules either sediment or diffuse, respectively. Therefore in order to ascertain an appropriate equilibrium speed the results of the SV analysis are often used, which through s can give an idea of the approximate size.

Once equilibrium is achieved, the shape of the macromolecule is no longer an important factor as there is no longer any net movement of the macromolecule within the cell, and no frictional resistance to flow. That shape of the macromolecule only affects the time taken to reach equilibrium. Therefore, from equilibrium runs the major factor that can be determined is the weight average molar mass (Van Holde & Baldwin, 1958).

The data gathered from the AUC, using either absorbance or Rayleigh interference optics, were analysed using the computer platform SEDFIT-MSTAR.v1. The algorithm employs the integral function M* of Creeth and Harding (1982)

$$M^*(r) = \frac{\big(c(r) - c(a)\big)}{kc(a).\big(r^2 - a^2\big) + 2k\int_a^r r\,[c(r) - c(a).dr]} \qquad (2.15)$$

where c(r) is the local concentration at radial position r, c(a) is the meniscus concentration, and k is the constant depending on the rotor speed, buffer density, the temperature and partial specific volume.

The M* function provides a convenient way of estimating the weight average molecular weight (M_w) over the whole macromolecular distribution in the cell from the identity of $M^*(r \rightarrow b) = M_w$, where b is the radial position at the bottom of the cell. By extrapolating the M* function to r=b we can obtain the M_w. Furthermore the SEDFIT-MSTAR algorithm evaluates the local weight average molecular weight at individual radial positions r (and hence local concentration c(r)) in the cell. These are obtained from the local slopes of the lnc(r) vs r^2 curves (Schuck et al., 2014). This also provides another method of obtaining the weight average over the whole distribution M_w from the "hinge point", the value of $M_w(r)$ when c(r) = the initial loading concentration, c. The values obtained for the M* and hinge point weight average molar masses should be similar to each other.

As with SV runs the data contains TI and RI noise, which are removed in the same way as to increase the resolution of the data. In addition to this distortion of the profiles can occur (through e.g. window imperfections at high speeds), in order to overcome this a baseline needs to be determined. This involves the recording of 5 initial scans taken as soon as the equilibrium speed has been attained and over a short period of time (~5 minutes) and averaging them, then repeating this process once the final equilibrium concentration distribution has been reached. The average initial scan is then subtracted from the average final scan, establishing a baseline with which SEDFIT-MSTAR works upon.

2.3.2 Apparatus

2.3.2.1 Analytical Ultracentrifuges

Sedimentation velocity and equilibrium experiments were conducted on a Beckman Optima XLI ultracentrifuges. The ultracentrifuges contain a vacuum chamber where the samples are placed, the use of a vacuum removes air and reduces air frictions reducing any temperature increases whilst running. The temperature of the chamber is set and maintained to within ±0.1°C. The drive unit within the ultracentrifuge has a top speed of 60,000rpm and can be fitted with one of two titanium rotors for runs, a 4 hole An-60Ti or 8 hole An-50Ti, which holds 3 or 7 cells respectively as well as an additional counterbalance cell.

The Beckman operating software ProteomeLab v6.2 is used to setup the AUC methods.

2.3.2.2 Analytical Cells

Sedimentation velocity experiments were predominantly carried out using two channel 12mm epoxy resin centrepieces and two sapphire windows on either side, enclosed within an aluminium case. The windows were placed into the aluminium case with plastic gaskets and an aluminium screw top. Sedimentation equilibrium experiments used longer aluminium cases that could accommodate a two port 20mm titanium centrepiece and sapphire windows. The windows were assembled in the same manner however an extra protective gasket was placed between the window and the titanium centrepiece, protecting the window.

Both cell types were tightened to a torque of 130lb and then filled. The 12mm cells generally had 400µL of sample injected into the left hand port and likewise with the buffer in the right side port. The 20mm cells employed the same method but used volumes of 150µL. Once filled, the sample injection ports were sealed with butyl rubber discs and aluminium screws.

2.3.2.3 Optical System

In order to analyse the movement of the macromolecules during centrifugation an optical measuring system was used. The system involves the use of a high precision monochromator that takes absorbance and Rayleigh interference measurements. All measurements were recorded and translated using ProteomLab v6.2.

As stated in 2.2.1 absorbance measurements are useful for macromolecules with chromophores, such as proteins or glycoproteins, as they absorb UV radiation. The absorbance optics measure along the path length of the cell, taking approximately 2 minutes for each cell. The data collected shows the intensity difference (absorbance) within the solution as the macromolecules start to sediment.

Rayleigh Interference measurements involve the use of monochromatic light as opposed to UV light as in absorbance. The interference measurements were made along the path length of the cell again, however the data is used to produce fringe patterns. The fringe patterns were optimised before the samples were spun at high speed. Optimisation typically took place at 3000rpm. Once optimised, the rotor speed was increased and measurements were taken. The sedimentation of the macromolecules produces a boundary within the cell between the sedimenting sample and the solvent, the change in boundary position within the cell is measured by the interference optics and relates to the sedimentation coefficient of the macromolecule.

3 Hydrodynamic Analysis of an Ovalbumin preparation

3.1 Introduction

Egg whites make up approximately 66% of the mass of eggs, it protects the egg yolk in early development and as a source of nutrition and protein for developing embryos. The main protein within egg white is ovalbumin, a glycoprotein constituting around 54% of the dry mass of the egg white (Mine, 1995). The function of ovalbumin is not fully understood, however it is thought it acts as a storage protein (Huntington et al., 2001)

Ovalbumin is a glycoprotein with a protein backbone consisting of 385 amino acids giving a molecular weight of 42.69 kDa, however the additional carbohydrates attached give an overall molecular weight of 44.29 kDa (Nisbet et al., (1981) & Tai et al., (1977)). However these values have slight variation between species.
The protein backbone of ovalbumin is bonded to the glycans through N-glycosidic bonds on residues containing amine groups. One such residue is asparagine (Asn) 292 which has been shown to form such linkages, another possible site that has been identified is asparagine 317 (Harvey et al., 2000 & Huntington et al., 2001). The composition of the glycans attached to ovalbumin have been shown to contain high levels of mannose (Man) and N-acetylglucosamine (GlcNAc) monomers, common structures found to be adopted include $(Man)_5(GlcNAc)_2$ and $(Man)_6(GlcNAc)_2$ (Neuberg (1938) and Tai et al. (1977)). Figure 3.1 shows the structure of one of the main glycans. The glycosylation of ovalbumin accounts for approximately 4% the dry weight of the molecule, therefore the protein is lightly glycosylated (Kiely et al. 1976).

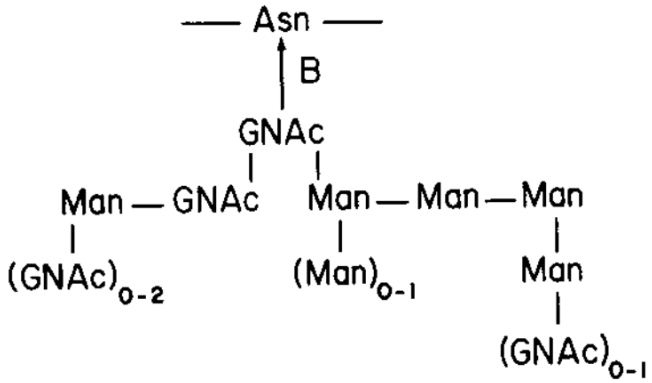

Figure 3.1: Main structural template of the N-linked glycans attached to ovalbumin, (GNAc = N-acetylglucosamine). Obtained from Kiely et al. (1976).

Although ovalbumin has a low level of glycosylation, the residues that are present may have a structural impact on the protein-protein level. N-acetylglucosamine is a mainly hydrophobic molecule which can form 'sticky patches' that can bind to other hydrophobic regions, allowing for the self-associations of macromolecules to occur (Ramakrishnan et al. 2012). Through these 'sticky patches' it is possible that ovalbumin can form weak dimers. A study by Ianeselli et al. (2010) showed that ovalbumin can readily form dimers in solutions of either no or very low salt concentrations.

3.1.1 Aim of Investigation

The aim of this part of the study is to use viscosity, sedimentation velocity and sedimentation equilibrium measurements to determine the hydrodynamic characteristics of a preparation of ovalbumin in terms of its heterogeneity.

3.2 Materials and Methods

3.2.1 Materials

A 1L phosphate buffered saline (PBS) solution of pH 7.0 was prepared using 2.923g sodium chloride, 1.561g dihydrogen potassium orthophosphate and 4.595g sodium dihydrogen dodecahydrate, obtained from Sigma Aldrich, UK.

Ovalbumin (98% purity) was purchased from Sigma Aldrich, UK. A 15mL 10mg/mL stock solution of ovalbumin was prepared using 150mg of ovalbumin and PBS buffer.

3.2.2 Ovalbumin sample preparation and concentration determination

A stock solution of ovalbumin at a nominal concentration of 10mg/mL in PBS buffer was prepared.

The concentrations of the samples was determined using a Cary-50 UV spectrophotometer, measuring at a wavelength of 280nm which was zeroed using PBS buffer. Prior to each measurement each concentration was diluted by taking 0.2mL of their respective stock and adding PBS to achieve their respective stock volumes, this gave a different dilution factor for each concentration. Diluted samples were then placed into reduced 1mL quartz cuvettes and placed into the spectrophotometer, readings were taken until 5 relatively close absorbance values were achieved.

Concentrations were determined using Equation 2.10, with an extinction coefficient of 660g/ml cm^{-1}, the absorbance value given was then multiplied by the dilution factor to give the stock concentration of each dilution.

3.2.3 Density and Viscosity Measurements

Density measurements were carried out using the 2mL extract of each concentration. Measurements were made using the Anton Paar DMA5000 density meter, following the method outlined in (2.1.2). The densities were recorded until 3 stable readings were obtained and averaged.

Viscosity measurements were conducted using an Ostwald capillary viscometer, using the 2mL extract of each concentration and the PBS buffer. The samples were

injected into the U-tube reservoir, 2mL, and placed into the water bath at 20°C. The flow times of the samples was recorded by the timing unit outlined in section 2.1.4.

3.2.4 Sedimentation Velocity

Sedimentation velocity analysis was carried out using the Beckman XL-I AUC. To reduce the effects of non-ideality a low concentration ovalbumin solution, 0.5mg/mL, was analysed.

The samples were loaded into the 12mm aluminium epoxy centrepiece XLI cells, a volume of 0.4mL 0.5mg/mL ovalbumin and 0.4mL of PBS buffer was loaded into each cell. The cells were inserted into the 4 hole rotor and then into the AUC set at 20.0°C. An initial rotor speed of 3000rpm was applied to check that all cells were fine and to allow the vacuum to be reached. A rotor speed of 45,000 rpm was used with measurements made using Rayleigh interference optics. Scans were taken at 2 minute intervals for each sample until 500 scans of each sample were acquired. The data was analysed using SEDFIT producing both ls-g*(s) and c(s) analysis (refer to section 2.3.1.1). Within the parameters a buffer density of 1.0032g/mL and a $\bar{v}$ value of 0.748mL/g were used (Harding, 1981).

3.2.5 Sedimentation equilibrium

Sedimentation equilibrium was carried out using the Beckman XL-I AUC, three 20mm titanium centrepiece cells were constructed. The cells were loaded with 0.15 mL of 0.5 mg/mL ovalbumin and 0.15 mL of PBS buffer.
The samples were centrifuged at 20,000 rpm over 3 days at 20°C, measurements were made using Rayleigh interference optics every 1 hour. The data was analysed using SEDFIT-MSTAR (Schuck et al., 2014), using the average if the final 5 scans (refer to section 2.3.1.2).

A subsequent SE run was performed in the same manner as before, however a 1.5mg/mL ovalbumin solution was examined. Both runs had the same parameters of 1.0032 g/mL for buffer density and a $\bar{v}$ of 0.748 mL/g.

3.3 Results and Discussion

3.3.1 Concentration measurements

The actual concentrations of the ovalbumin solutions were determined through spectrophotometry, using Equation (2.10) and multiplying the result by the relevant dilution factor. The extinction coefficient used for ovalbumin was 660 $mL.g^{-1}.cm^{-1}$. The values obtained for the actual concentrations were very close to the weighed out nominal concentrations, Table 3.1 shows the results and calculated actual concentrations of the samples.

Figure 3.1: Absorbance readings for ovalbumin solutions and subsequent determination of actual concentrations.

	Absorbance Readings							
Nominal conc (g/mL)	1	2	3	4	5	Average	DF	Actual conc (g/mL)
0.01	0.0871	0.0875	0.0872	0.0880	0.0877	0.0875	75	0.0099
0.009	0.0915	0.0909	0.0913	0.0911	0.0910	0.0912	65	0.0089
0.008	0.0921	0.0922	0.0914	0.0919	0.0915	0.0919	55	0.0077
0.007	0.0916	0.0914	0.0916	0.0913	0.0911	0.0915	45	0.0062
0.006	0.1034	0.1033	0.1032	0.1031	0.1032	0.1032	35	0.0055
0.005	0.1279	0.1284	0.1284	0.1282	0.1280	0.1282	25	0.0049

3.3.2 Density and Viscometry

Density measurements were recorded for the ovalbumin concentrations and PBS buffer, these were used to calculate the density correction ratio (ρ/ρ_0) for the determination of the intrinsic viscosity. The densities and correction values for each concentration are laid out in Table 3.2.

Table 3.1: Density measurements for varying concentrations of ovalbumin in PBS at 20.0°C

Nominal concentration (g/mL)	Readings (g/mL)			
	1	2	Average	ρ/ρ_0
0.01	1.00576	1.00577	1.00576	1.003457
0.009	1.00538	1.00541	1.00539	1.003090
0.008	1.00484	1.00452	1.00468	1.002374
0.007	1.00467	1.00467	1.00467	1.002363
0.006	1.00380	1.00390	1.00385	1.001545
0.005	1.00345	1.00346	1.00345	1.001149
PBS	1.00326	1.00135	1.00230	

The flow times of the ovalbumin solutions were used to determine the relative, reduced and inherent viscosities using Equations (2.3, 2.4 & 2.5) respectfully, refer to Table 3.3 for values.

Table 3.3: relative, reduced and inherent viscosities of ovalbumin in PBS at 20.0°C

Nominal concentration (g/mL)	Relative viscosity, η_r (mL/g)	Reduced viscosity, η_{red} (mL/g)	Inherent viscosity, η_{inh} (mL/g)
0.01	1.06	6.11	5.93
0.009	1.05	6.05	5.86
0.008	1.04	5.76	5.64
0.006	1.03	5.96	5.87
0.005	1.02	5.24	5.18

Using the reduced and inherent viscosities plotted against actual concentration and extrapolated to zero concentration the intrinsic viscosity was found to be (5.0± 0.15) mL/g, and Figure 3.2 shows the extrapolation determination. According to studies by Koseki et al. (1989) the intrinsic viscosity value for (monomeric) ovalbumin is between 4.2 – 4.5 mL/g.

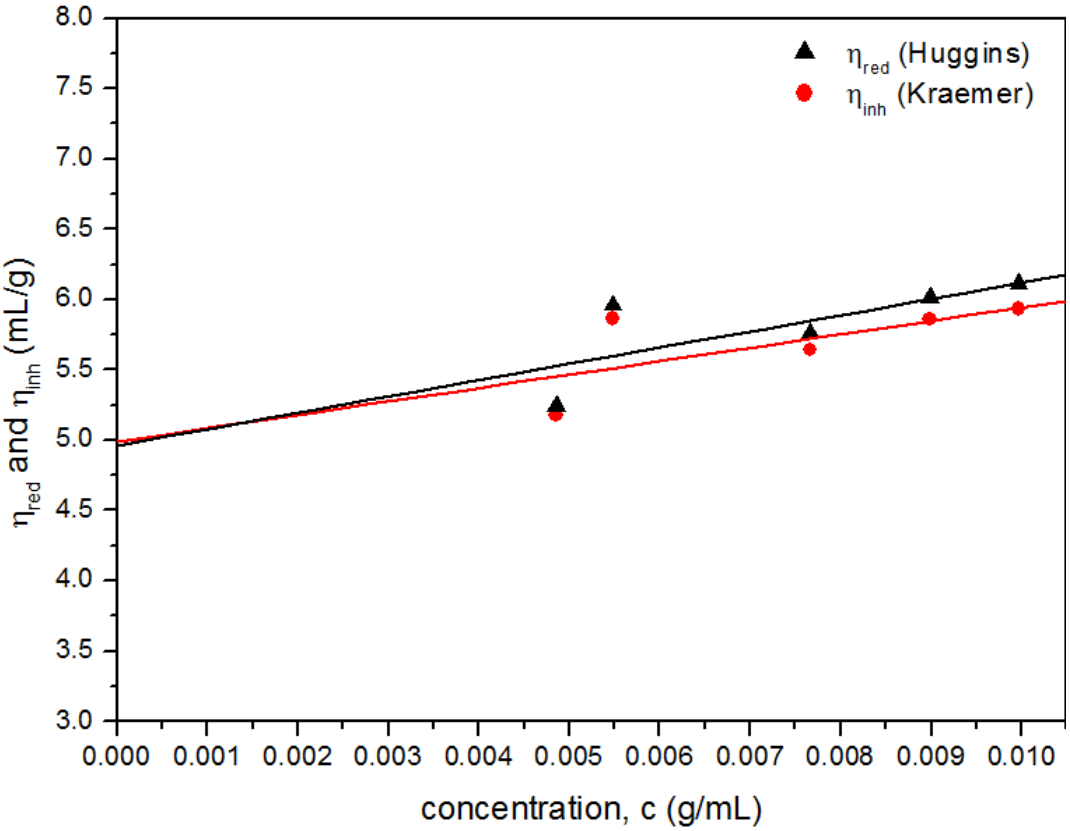

Figure 3.2: Extrapolation to zero concentration of reduced and inherent viscosities of ovalbumin at 20.0°C. The y-intercept is the intrinsic viscosity value [η].

The larger value obtained through this study can be attributed to heterogeneity within the ovalbumin sample, possibly due to the presence of some dimers. This is borne out by the sedimentation velocity results.

3.3.3 Sedimentation Velocity

The data from the sedimentation velocity run for the ovalbumin was analysed using SEDFIT, the results of the run are shown in Figure 3.3. The top plot shows the ls-g*(*s*) against s distribution, the bottom plot shows the c(*s*) against *s* distribution.

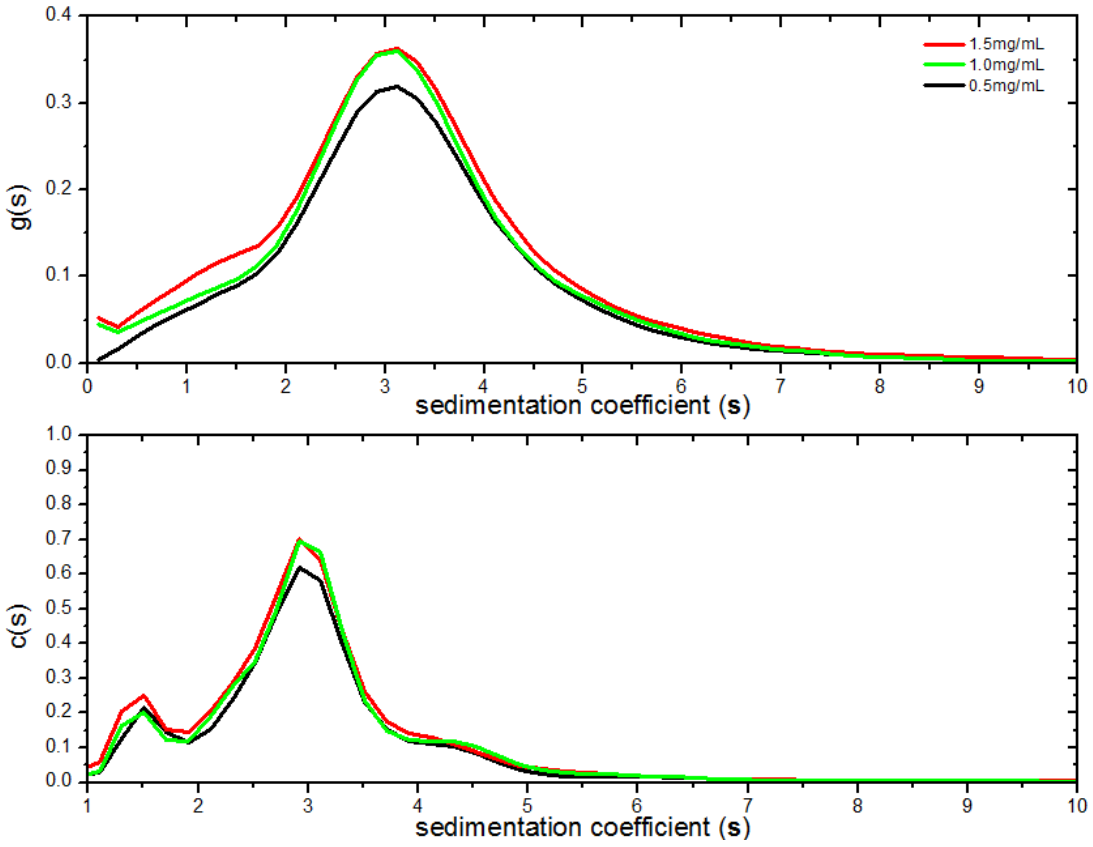

Figure 3.3: Sedimentation velocity analysis for ovalbumin concentration series. Top: ls-g*(*s*) analysis. Bottom: c(*s*) analysis.

The distribution results from the ls-g*(s) plot shows that the ovalbumin solutions are predominantly monodispersed, this is indicated through the appearance of only 1 main peak at (3.2± 0.3) S. The main peak at 3.2 S makes up approximately 92% of the total signal, indicating that the macromolecule responsible for the peak makes up ~92% of the solution. The sedimentation coefficient obtained from the study is very similar to values obtained from Polson et al. (1967), the study showed that ovalbumin has a sedimentation coefficient of 3.15 S at 42,000 rpm. This value is very similar to the value obtained in this study. However the g(*s*)

vs *s* and c(*s*) plots show significant amounts of low molecular weight contaminants (*s*~1.5S) and what appears to be a dimer (*s* ~ 4.5 S).
The lower plot of Figure 3.3 shows the c(*s*) distribution of ovalbumin. As stated in 2.3.1.1 c(*s*) analysis includes diffusion within the algorithm giving more defined peaks, when applied to this data the single peak shown by the ls-g*(*s*) analysis shows that it is composed of 3 peaks; Peak 1 (1.5 S), Peak 2 (3.2 S) and Peak 3 (4.5 S). Peak 1 at 1.5 S is likely a result of undialysed small molecular weight contaminants

Peak 2 on the distribution is relatively narrow with defined ends yielding an *s* value of approximately 3.2 S. The sedimentation coefficient supports the sedimentation coefficient value obtained ls-g*(*s*) distribution, as well as falling within the limits of the study conducted by Polson et al. (1967). The *s* value also indicates that the majority of the material in solution is monomeric ovalbumin.

Peak 3 although small, indicates that there are molecules present with a sedimentation coefficient of ~4.5 S. The main explanation for this is that some of the ovalbumin has formed dimers, as stated in 3.1 the likely occurrence for dimerisation is the bonding of two 'sticky patches' on ovalbumin monomers. As shown in the study by Ianeselli et al. (2010) at low salt concentration ovalbumin can form dimers, from the c(*s*) distribution it is evident that the 0.1M PBS buffer is sufficiently low enough to allow low level of dimerisation.

3.3.4 Sedimentation Equilibrium

Sedimentation equilibrium data was analysed using SEDFIT-MSTAR for all samples. As stated in 2.3.1.2 a baseline was established in SEDFIT-MSTAR by subtracting the first 5 initial scans from the last 5 scans, the baseline corrected data was then used to determine the molar mass. Figure 3.4 shows the 4 plots based upon the SEDFIT-MSTAR algorithm (Schuck et al., 2014) for one of the 0.5 mg/mL ovalbumin samples; they show ln(c) vs r^2, M* vs r and $M_{W,app}(r)$ vs r or c(r).

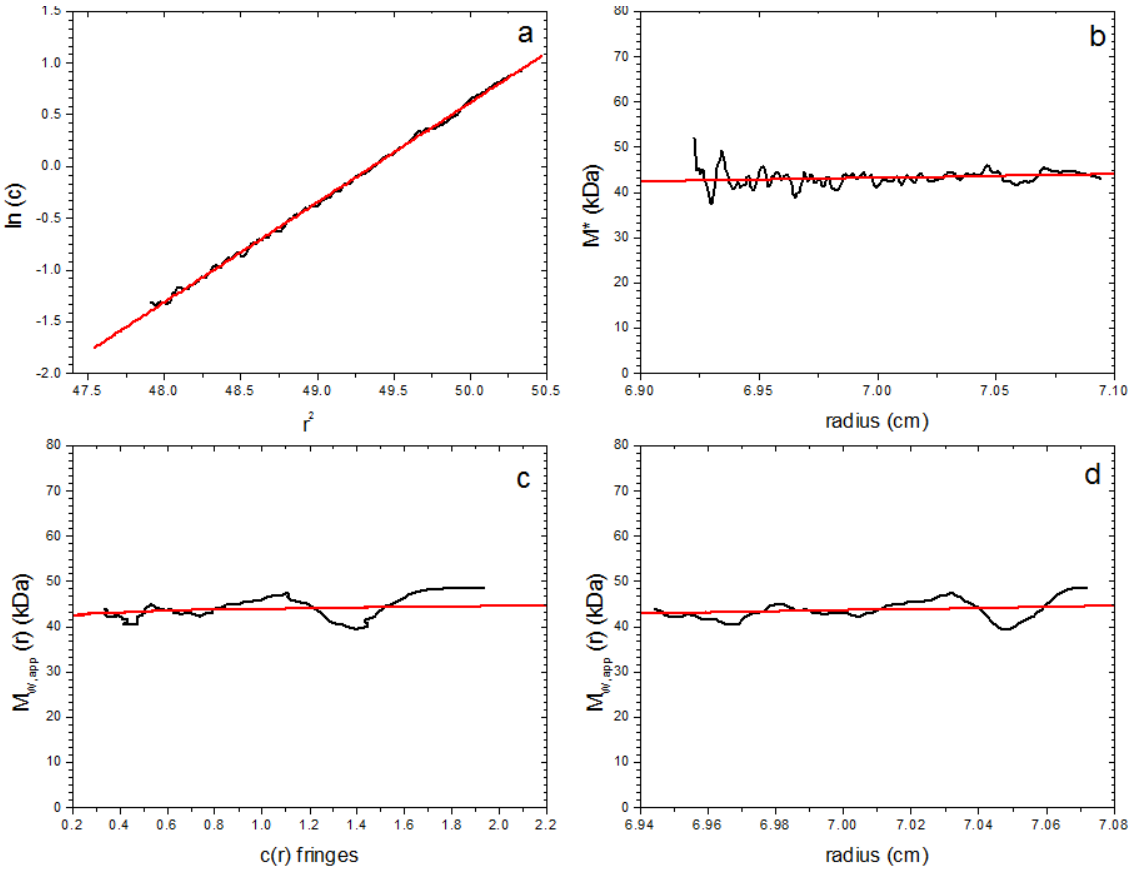

Figure 3.4: Molar mass analysis for 0.5 mg/mL ovalbumin from SEDFIT-MSTAR: (a) log of concentration in the cell vs the square radial displacement, (b) M* analysis vs radius, (c) point average molecular weight vs local concentration c(r) in the ultracentrifuge cell, (d) point average apparent molecular weight vs radial position in the cell.

The data shown in Figure 3.4 shows not only the molecular weight of the ovalbumin but other factors as well. Plot (a) show the natural logarithm of the data against the square of the radius. The raw data (black) and the fitted data (red) lay directly on top of each other, this is an indication that the sample is predominantly monodispersed. There is a small degree of noise on the data that suggests other molecules are present.

Plot (b) shows the M* analysis plot. The weight average molar mass over the whole distribution is obtained from extrapolating the M* function to the cell base (Creeth & Harding, 1982), using the identity $M^*(r \rightarrow b) = M_w$. A value of (44.6±1.5) kDa is obtained.

Plots (c) and (d) show the molecular weight apparent as a function of loading concentration and radius, respectfully. Both plots show a similar weight of approximately 45kDa, both the raw and fitted data shows a flat line indicating the sample is again monodispersed. Similar to the M* plot (b), there is noise within the data indicating that there is extra material within the sample other than monomeric ovalbumin.
Using the data from the $M_{w,app}$ (r) vs r and $M_{w,app}$ (r) vs c(r) plots the hinge point molecular weight can be calculated, for this sample the value was calculated to be approximately 45.7kDa. The value obtained is very similar to the value obtained from the determination of M_w from the M* plot. The whole distribution Mw values obtained at loading concentrations of 0.5mg/mL (3 repeats) and 1.0mgmL (repeats) from the M* and hinge methods are compared in Table 3.4.

Table 3.2: Summary of weight average M_w results for 0.5 and 1.0 mg/mL ovalbumin samples, centrifuged at 20,000rpm.

Sample concentration (mg/mL)	0.5 (1)	0.5 (2)	0.5 (3)	1.0 (1)	1.0 (2)	1.0 (3)
M_w (kDa) - from M*	45.2	45.4	45.1	44.1	43.6	43.9
M_w (kDa) - from hinge point	45.7	45.6	45.5	44.9	44.8	44.7

The results show that despite the presence of low molecular weight contaminants (totally ~8% as evident from the sedimentation velocity analysis), the overall weight average molecular weight for ovalbumin is close to the sequence value for the molar mass of ovalbumin (44.3kDa)

3.3.5 Shape Determination

The ELLIPS1 algorithm of Harding et al (2005), Harding and Garcia de la Torre (2013) was used in the shape determination.
The first parameter that needs to be determined is the swollen specific volume (v_s) this is derived using Equation (3.1).

$$vs = \frac{\bar{v} + \delta}{\rho_0} \qquad (3.1)$$

where $\bar{v}$ was taken as 0.748 mL/g, ρ_0 (solvent density) was 1.0023 and δ was the hydration of ovalbumin. The value for the hydration was derived from a study by Harding (1981) which used a hydration value of 0.57. Using the values of the experiment and Equation (3.1) a v_s of 1.32mL/g.
The determination of the Perrin function were calculated used BIOMOLS2 (Gillis, private comm.), which required several parameters; $\bar{v}$, v_s, ρ_0, the frictional ratio (f/f_0) determined using the sedimentation coefficient, and

the hydration δ. Using these values and BIOMOLS2 a Perrin value of 1.091 was obtained. This value was compared to the value obtained by Harding (1981) who obtained a slightly lower value of 1.033.
The Perrin values were then inserted into ELLIPS1 and the axial ratios were obtained, Figure 3.4 shows the results of the analysis.

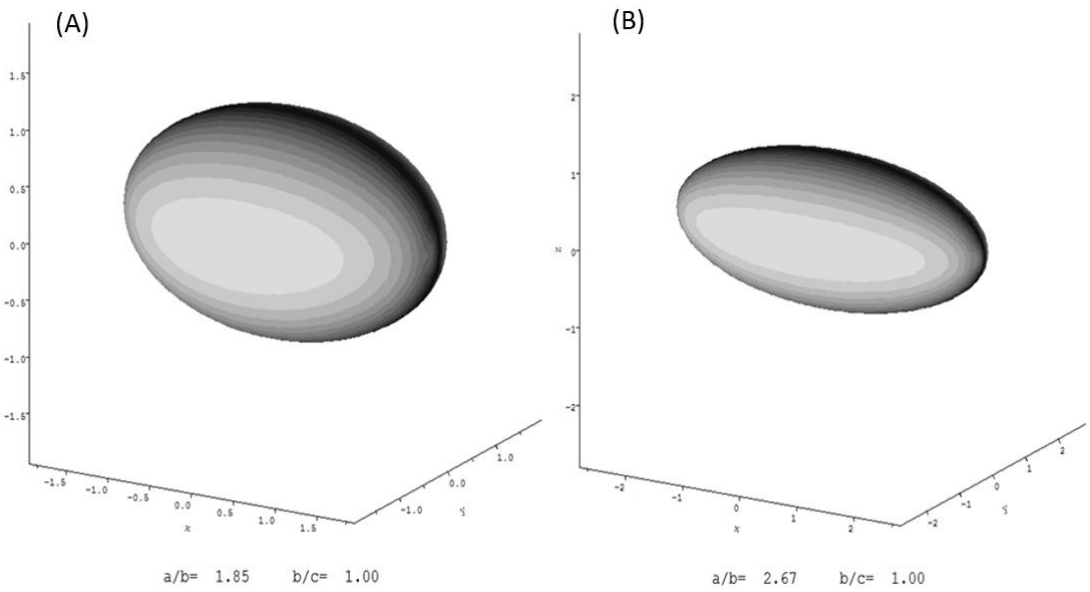

Figure 3.5: Prolate models of ovalbumin with axial ratios. (A) Shape obtained from Harding (1981) study. (B) Shape determined from results of this investigation.

Figure (3.4, A) shows the structure obtained from Harding (1981) which shows a prolate model with an axial ratio of 1.85:1. The shape shown in (3.4, B) shows a similar shape in that a prolate structure is indicated by the data, however the axial ratio is larger (2.7:1).

As stated the Perrin function is derived using several parameters including the frictional ratio, this is obtained using data including the sedimentation coefficient. The result of the investigation showed that ovalbumin had an *s* value of ~3.2 S, whereas the study by Harding (1981) showed a sedimentation coefficient value of 3.38 S for ovalbumin. Therefore the differences in sedimentation coefficients will yield different frictional ratios which will affect the Perrin value, thus leading to different axial ratios.

The sedimentation coefficient obtained from this study was shown to have been impacted by the presence of partially degraded ovalbumin and dimeric ovalbumin, therefore the difference in value to Harding (1981) can be attributed to this. Had the sample not contained these contaminants the resulting axial ratio would have been closer to the 1.9:1 ratio.

3.4 Conclusion

The characterisation of ovalbumin involved the use of viscometry, density measurements, sedimentation velocity and sedimentation equilibrium measurements in order to determine the hydrodynamic properties of ovalbumin.

The analysis methods showed that ovalbumin had an intrinsic viscosity of approximately 4.9mL/g which was higher than previous studies had indicated, however this was attributed to the presence of lower and higher molecular weight contaminants present.

The sedimentation velocity g(*s*) data showed a large average peak at 3.2S, however there was an indication of extra material being present. The c(*s*) distribution indicated the main peak again at 3.2 S for monomeric ovalbumin, however there were also a peaks at both 1.5 S and 4.5 S which were indicative of degraded and dimeric ovalbumin respectively.

Finally the sedimentation equilibrium data showed that the molecular weight of ovalbumin at a concentration of 0.5mg/mL was approximately 45kDa, which corresponds to the actual molecular weight of ovalbumin.

4 Evidence of Vancomycin dimerisation and interactions with mucin

4.1 Introduction

Glycopeptides are a type of glycan with generally lower molecular weights that glycoproteins such as ovalbumin, glycopeptide antibiotics against serious diseases are like this. In essence, they are similar to glycoproteins composed of amino acids with glycans covalently bonded, however they are often much smaller; being composed of several amino acids bound frequently to oligosaccharide residues (Reynolds, 1989).

Vancomycin is a antibiotic glycopeptide that is used to treat gram-positive bacterial infections, such as methicillin-resistant *Staphylococcus aureus* (MRSA) and *Enterococcus* species (Small et al., 1990). It is often a 'last resort' treatment due to the its potency and adverse side effects such as loss of hearing and possible kidney failure. The emergence of MRSA has led to vancomycin becoming administered more as a treatment. This increase in administration has led to the discovery of vancomycin-resistant cases (Gardete & Tomasz, 2014).

Vancomycin is a small glycopeptide with a molecular weight of 1449Da, it is a member of the heptapeptide glycopeptide family as it is composed of seven modified amino acids joined to the vancosamine-glucose disaccharide (Jia et al., 2013). Figure 4.1 shows the structure of vancomycin with the seven amino acids highlighted and numbered; (1) N-methyl-D-leucine, (2 & 6) m-chloro-β-hydroxy-D-tyrosine, (3) asparagine, (4) D-phenyl glycine, (5) p-hydroxy-D-phenylglycine and (7) m,m-dihydroxy-L-phenylglycine.

The glycan residue of vancomycin, vancosamine-glucose, is attached to the main peptide backbone through O-linked glycosidic bonds (Barna & Williams, 1984). The O-linkages are different to N-linkages seen in earlier in ovalbumin. Here, the oxygen of the glycosidic bond remains and is not replaced as for N-linkages.

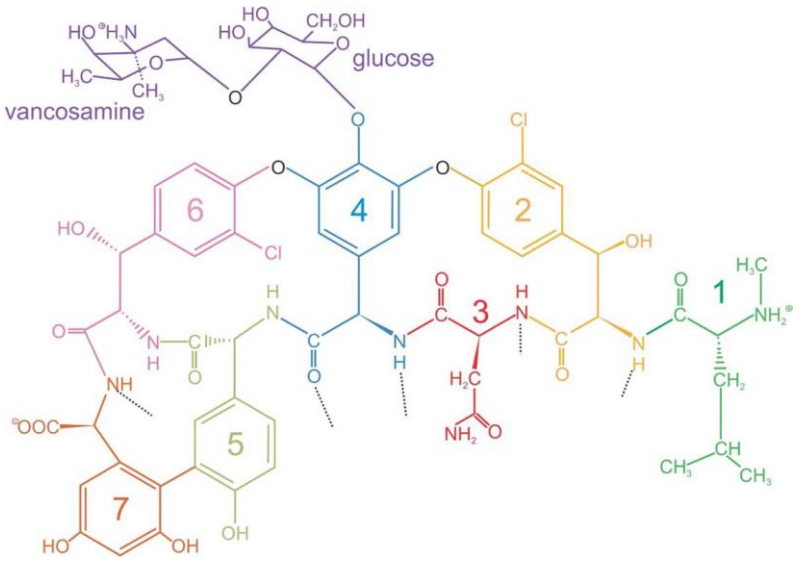

Figure 4.1: Structure of vancomycin with numbered residues, see above. The disaccharide subunit is bound to residue 4 (purple) (Loll et al., 1998).

The antibiotic mechanism through which vancomycin works is by binding to peptidoglycan precursor molecule on bacterial cell walls. This binding inhibits further synthesis of peptidoglycan resulting in a weak cell wall that can eventually burst as the bacteria grows (Yim et al., 2014).

The terminal end of the peptidoglycan precursor consists of a D-alanyl-D-alanine (D-Ala-D-Ala) residue, this D-Ala-D-Ala groups forms several hydrogen bonds with the vancomycin. The binding of vancomycin to the D-Ala-D-Ala results in an inhibition of transpeptidation and transglycosylation of the peptidoglycan precursor, reducing the levels of cross-linking between the peptidoglycan resulting in weak, less rigid cell wall (Nieto & Perkins, (1971a), Binda et al., (2014) & Williams et al., (1999). The binding of vancomycin to the D-Ala-D-Ala residues has been reported to occur as a dimer, whereby the binding of dimeric vancomycin to one residue increases the chance of vancomycin binding to another D-Ala-D-Ala residue (Loll et al., 1998). However, these studies have looked at the dimerisation of vancomycin in the presence of the D-Ala-D-Ala peptidoglycan residues or similar structure. The first part of this

investigation explored the dimerisation of vancomycin in the absence of a possible ligands in several different buffer conditions, including a medical buffer. Using SE analysis the dissociation constant of dimeric vancomycin was determined. The results were compared to previous studies which determined the values in presence of the ligand. SV analysis of vancomycin is not possible owing to the low molecular weight of vancomycin. This would involve rotor speeds in excess of 50,000rpm which are not practical or safe with the equipment available.

The second part of this study investigated the possible interaction of vancomycin with gastric mucins (GM).

As stated, vancomycin is an effective antibiotic that's use is minimised in order to reduce antibiotic resistance and possible harmful side effects. The normal administration procedure is to inject a solution of vancomycin at a concentration of between 2.5 - 5.0 mg/mL in a 0.9% NaCl solution intravenously. The reasoning being to obtain an entry time of the vancomycin at approximately 10mg/min (van Hal et al., 2013). This method is preferred to oral administration as the absorption of vancomycin within the intestine is poor, resulting in administrations of roughly 125mg four times a day. It has been reported that adverse side effects such as indigestion often occurs (Cataldo et al., 2012). The reason why vancomycin is poorly absorbed is not fully understood, therefore tin order to overcome this issue orally administered vancomycin must be taken 3 - 4 times a day at in 500mg doses (Rybak et al., 2009).

In cases where vancomycin is orally administered vancomycin enters the gastrointestinal (GI) tract, where it comes into contact with many different macromolecules. The resulting interactions with these macromolecules may result in the poor absorption of the vancomycin. One of the most common macromolecules that vancomycin is likely to interact with are gastric mucins (GM). They are abundant within the GI tract due to the lubrication and mucoadhesive properties (Gillis et al., 2013). Gastric mucins are large glycoproteins with very high levels of glycosylation, their molecular weights range commonly between 500kDa – 20MDa. The protein backbone of mucin typically makes up approximately 20% of the molar mass while the remainder (~80%) is normally representative of the attached glycans (Bansil & Turner, 2006). Due to the high levels of

glycosylation mucins adhere to most molecules within the GI tract through hydrogen bonds, hydrophobic and hydrophilic interactions (Harding et al., 1999).

On this basis this investigation looked at the interaction between gastric mucin, specifically porcine gastric mucin (PGM) from pigs as it is similar to the human homolog (HGM) and often used as a model for HGM (Kararli, 1995). Using SV analysis the study will determine whether vancomycin interacts with PGM and, if so, what implications this would have on the oral administration of vancomycin.

4.1.1.1 Aims of the Investigation

This investigation has two main aims. Firstly to look at the dimerisation of vancomycin in the absence of a ligand, and to determine the resulting dissociation constant from SE analysis. The second aim is an interaction study between vancomycin and PGM to determine if this could be a possible reason for the low absorption of vancomycin through oral administration.

4.2 Materials and Methods

4.2.1 Materials

Several 1.0L buffers were prepared that consisted of different conditions; (A) 10mM HEPES buffer (pH 7.9), (B) 10mM HEPES buffer & 100mM NaCl (pH 7.9), (C) 10mM HEPES buffer & 100mM NaCl & 20% glycerol (pH 7.9) and (D) 0.9% NaCl in water. The latter buffer condition is the normal conditions in which vancomycin is administered, the concentration of vancomycin being between 2.5-5.0mg/mL.

Two samples of vancomycin hydrochloride (powder) were supplied: one from Duchefa Biochemie, Haarlem, The Netherlands, the other from Sigma Aldrich, UK. They had a purity of 95% and 98%, respectively. The porcine gastric mucin type III (PGM) was supplied by Sigma Aldrich, UK.

4.2.2 Sample Preparations

Samples of vancomycin (Duchefa) were prepared in all four solvent conditions (A, B, C & D) to a stock concentration of 10.0 mg/mL, prepared by adding 15.0mg of vancomycin to 15.0 mL of each respective buffer type. Using each stock solution, a subsequent dilution series was created for each buffer condition. The dilutions consisted of concentrations of 5.00, 2.50, 1.25 and 0.60 mg/mL vancomycin. Once prepared the samples were stored at a low temperature within a refrigerator to prolong the stability of the vancomycin.

A separate Sigma vancomycin solution was prepared in 0.9% NaCl to a concentration of 50.0 mg/mL. Using the 50.0 mg/mL stock a dilution series was produced with concentration of; 40.0, 30.0, 24.0, 20.0, 12.0, 10.0 & 6.0 mg/mL vancomycin.

4.2.3 Vancomycin $\bar{v}$ and concentration determination

The conventional method for determining concentration is to use either spectrophotometry or refractometry, however in the case of vancomycin this was not possible as neither the extinction coefficient nor refractive increment were known. Therefore, in order to determine concentration

density measurements were carried out, as explained in section 2.1.1. In order to determine the concentration using equation (2.2), the $\bar{v}$ of vancomycin had to be determined.

The determination of the $\bar{v}$ for vancomycin was calculated using work carried out by Durchschlag and Zipper (1994). This method allows the $\bar{v}$ to be calculated based upon the structure of the molecule, in this case vancomycin. The method involves determining the partial molar volume ($\bar{\mathbf{V}}\boldsymbol{i}$), of given atoms or groups of atoms within a certain environment, within a given area of the molecule. Figure 4.2 shows the atoms that were taken into account.

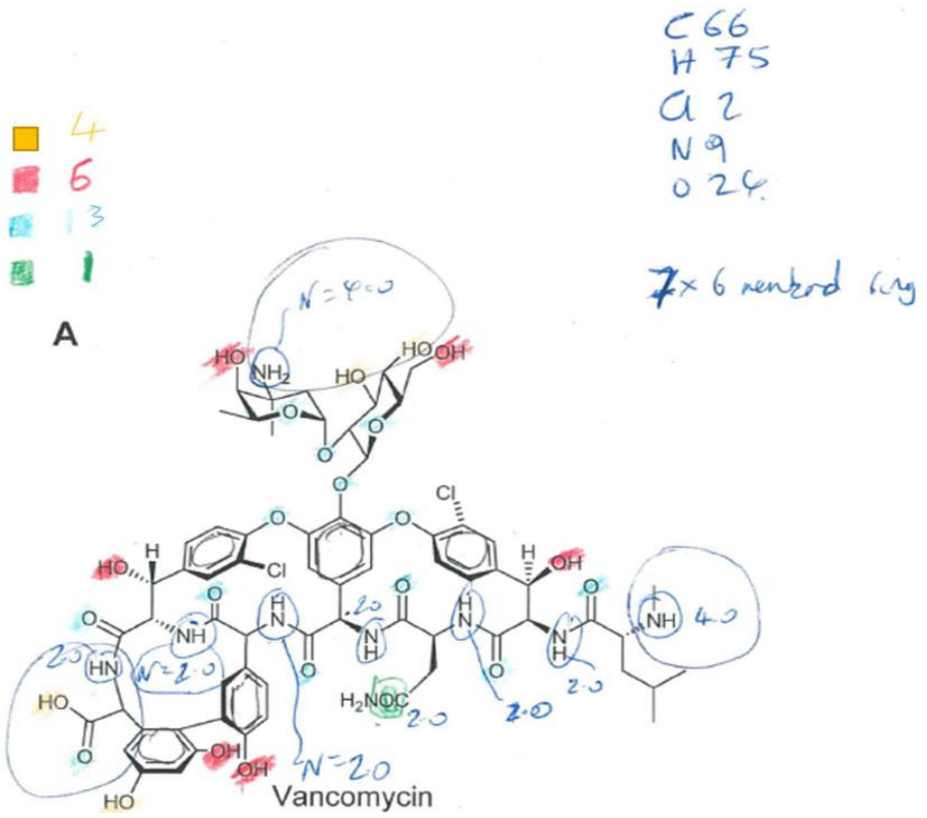

Figure 4.2: Structure of vancomycin with the different atomic environment highlighted. The number of each given atom is also indicated (top right).

Using the Durchschlag and Zipper $\bar{\mathbf{V}}\boldsymbol{i}$ values for each atomic environment and the number of each atom in each environment, an overall weighted average $\bar{\mathbf{V}}\boldsymbol{i}$ for vancomycin was obtained. The overall $\bar{\mathbf{V}}\boldsymbol{i}$ was combined

with a correction value, calculated based upon the covolume, ring formation and ionisation of the vancomycin, to give a correct value. The main parameter of importance was the charge of vancomycin at pH 7.9. A study by Johnson & Yalkowsky (2006) showed that at pH 7.9 the charge on vancomycin was +1.
Using these values the $\bar{v}$ of vancomycin could be calculated using Equation (4.1).

$$\bar{v} = \frac{\overline{\mathbf{V}}\boldsymbol{i}}{M} \qquad (4.1)$$

Where ($\bar{v}$) is the partial specific volume (mL/g), ($\overline{\mathbf{V}}\boldsymbol{i}$) is the corrected partial molar volume of vancomycin (979.20 mL/mol) and (M) is the molar mass of vancomycin (1449.25 g/mol). Using equation (4.1) the $\bar{v}$ for vancomycin was determined to be 0.67 mL/g.

Once the $\bar{v}$ was determined the concentration of the stock solutions could be calulated. For each solvent condition an equal amount of vancomycin was weighed out each time, therefore the concentration of one buffer (HEPES alone) was calculated as it would be representative of all conditions. The method outlined in section 2.1.2 was adopted with three density readings taken for both the solvent, the stock and first dilution with the results recorded in Table 4.1.

4.2.4 Viscosity Measurements

Viscosity and density measurements were recorded for each of the concentrations derived from the 50.0mg/mL dilution series in 0.9% NaCl.
Density measurements were carried out in the same way as in 2.1.2 using the Anton Paar DMA5000 oscillating capillary meter to determine the density correction ratio (ρ/ρ_0).
Viscosity measurements were conducted using the method outlined in 2.1.4, whereby 2.0 mL of a given concentration was placed into the U-tube and placed into the water bath at 20.0°C. The samples were then pumped up to the measuring reservoir and allowed to flow back down, with the flow times recorded in Table 4.2.

4.2.5 Sedimentation Equilibrium of vancomycin

SE runs were carried out using the Beckman XL-I AUC using 12mm aluminium cases and epoxy centrepiece cells. A total of four runs were carried out, with each solvent conditions being used per run.
The samples were loaded into the cells with 0.1mL of sample placed into one sector and 0.1mL of buffer placed in the other sector. The cells were then placed into the 8 hole Ti rotor and placed into the AUC set at 7.0°C, fringe adjustment was made at 3000 rpm after which a rotor speed of 47,500 rpm was applied. The cells were centrifuged at this speed for three days with Rayleigh interference optics taking readings every hour.

4.2.6 Vancomycin and mucin sample preparation

A stock solution of 10mL PGM at 5.0mg/mL was prepared using 0.9% NaCl. The solution was filtered using a Whatman Puradisc 30 cellulose acetate syringe filter with a 0.45µm cut off. The sample final concentration was then checked using the refractometer, with a dn/dc value of 0.165 mL/g being used in the calculations (Jumel et al., 1996). Using the concentration determined from the refractometer the stock solution was diluted down to 4.0 mg/mL. A stock solution of 5mL vancomycin (Sigma Aldrich) with a concentration of 25 mg/mL was prepared in a buffer of 0.9% NaCl. Using both stock solutions a 1:1 dilution was made by combing equal volumes of the vancomycin and PGM together. This resulted in a solution composed of vancomycin and PGM at concentrations of 12.5 and 2.0 mg/mL respectively.
In addition to this, a separate study looked at lower concentrations of vancomycin being added to PGM. 25.0 mg/mL stock solution was diluted 10-fold twice, yielding concentrations of 2.50 and 0.25 mg/mL. When combined with an equal volume of PGM, final concentrations were 1.25 and 0.125 mg/mL.

4.2.7 Sedimentation Velocity

SV runs were carried out using the Beckman XL-I AUC, using 12mm aluminium epoxy centrepiece cells. Data analysis was carried out using SEDFIT(15b), parameter values of 1.0032 g/mL and 0.64 mL/g were used for buffer density and $\bar{v}$ respectively.

The samples were loaded into the XLI cells. 0.4 mL of the 0.9% NaCl buffer was injected into one sector of each cell and 0.4 mL of the sample was injected into the other sector. Five cells were used, 3 contained a solution of 12.5 mg/mL vancomycin with 2.0 mg/mL PGM, 1 contained 2.0 mg/mL mucin alone and the last cell contained just water. The cells were then placed into an 8 hole rotor set at 20.0°C, with a speed of 3000 rpm applied to adjust the fringes. Measurements were made at a rotor speed of 30,000 rpm with Rayleigh interference optics for 12 hours, with scans taken every two minutes for a total of 500 scans. After the run was finished the cells were removed and examined. The examination revealed a thick layer of sedimented molecules. Analysis of the results on SEDFIT found that there was no sedimenting molecules present in the sample containing both PGM and vancomycin. It was hypothesised that these molecules sedimented immediately at the high speed. A further experiment was conducted whereby the samples were centrifuged at a much lower rotor speed of 3000 rpm at 20.0°C for 12 hours with Rayleigh interference optics being used every 2 minutes.

An additional SV run was carried out on the 12.5 mg/mL and diluted vancomycin solutions (1.25 & 0.125 mg/mL) with PGM added. The samples were placed separately into three XLI cells, with a reference sample of 0.9% NaCl also added. The samples were placed into the XL-I centrifuge at a temperature of 20.0°C. A rotor speed of 3000 rpm was applied and interference optics took readings every two minutes for five hours. After this period the rotor speed was increased to 30,000 rpm for 12 hours, again with interference readings every two minutes. The reason for the increase was to determine if there was any non-aggregated mucin present.

4.3 Results and Discussion

4.3.1 Concentration measurements

The results of the density measurements for the 10 mg/mL stock vancomycin and the first dilution (5 mg/mL), showed that the nominal concentrations were very close to the actual concentrations (refer to table 4.1). Using Equation (2.2) and a $\bar{v}$ value of 0.67 mL/g the concentration of the stock solution was calculated to be 9.8 mg/mL and the first dilution was 4.9 mg/mL.

Table 4.1: **Determination of actual concentration from density measurements for 10.0 & 5.0 mg/mL vancomycin solutions at 20.0°C.**

Nominal concentration (mg/mL)	Average Density (g/mL)	Actual concentration (mg/mL)	Actual concentration (g/mL)
10.0	1.002440	9.8	0.0098
5.0	1.000831	4.9	0.0049
solvent	0.9992	-	-

The concentrations indicated from the density measurements show that actual and nominal values are accurate to one another. The slightly lower values from the actual concentration can be attributed to the hydration of the sample.

Due to the closeness of the nominal concentration to the actual concentration it can be reasonably assumed that the rest of the vancomycin buffer conditions have the same concentrations, as they were all made using the same weight of vancomycin. The determination of an accurate concentration is important for AUC analysis and in the calculation of the dissociation constants, as the concentration can have a large impact.

4.3.2 Viscosity measurements

Density and viscosity measurements were made for all the vancomycin dilutions made from the 50.0 mg/mL 0.9% NaCl "medical" solvent.
Solution density measurements were made in each case to determine the actual concentration and to correct the viscosity values due to the high concentration. Table 4.2 shows the density readings and the density correction ratio (ρ/ρ_0) along with the actual concentration of each dilution determined using equation (2.2).

Table 4.2: Density measurements at 20.0°C for each nominal dilution with the density correction (ρ/ρ_0) and actual concentration calculated.

Nominal concentration (mg/mL)	Average Density (g/mL)	ρ/ρ_0	Actual concentration (mg/mL)
50	1.02045	1.01582	48.6
40	1.01750	1.01289	39.6
30	1.01417	1.00957	29.4
24	1.01239	1.00780	23.9
20	1.01108	1.00649	19.9
12	1.00847	1.00389	11.9
10	1.00779	1.00322	9.9
6	1.00648	1.00192	5.9
0.9% NaCl	1.00456	-	-

The results shown in Table 4.2 show that the nominal concentrations are close to actual concentrations, they are within the range of ~3% similar to the results shown in 4.3.1. As stated earlier this slight decrease in actual concentration can be accounted for through the hydration of the vancomycin. The values for ρ/ρ_0 are all above 1.0 which indicates that all the dilutions have a greater density than the buffer and as a result will determine a more accurate intrinsic viscosity value.

The viscosity of vancomycin was determined using the flow times of the vancomycin dilutions through an Ostwald capillary viscometer. The results of the flow times were used to determine the relative viscosity using Equation (2.3), the density correction ratios and actual concentrations in Table 4.2. Using the relative viscosity the subsequent reduced and inherent viscosities were calculated using Equations (2.4 & 2.5) respectively. The values for all three viscosities can be seen in Table 4.3 along with the average flow times.

Table 4.3: Average flow times at 20.0°C for each concentration along with the subsequent relative, reduced and inherent viscosities.

Nominal concentration (g/mL)	Average flow time (s)	Relative viscosity, η_r	Reduced viscosity, η_{red} (mL/g)	Inherent viscosity, η_{inh} (mL/g)
0.050	109.53	1.180	3.709	3.410
0.040	105.61	1.135	3.404	3.193
0.030	102.63	1.099	3.370	3.213
0.024	100.41	1.074	3.064	2.957
0.020	99.41	1.061	3.076	2.985
0.012	97.34	1.037	3.058	3.003
0.010	96.43	1.026	2.651	2.617
0.006	95.52	1.015	2.576	2.557

The results of the reduced and inherent viscosities in Table 4.3 show a general decrease as the concentration reduces. Using these values the intrinsic viscosity of vancomycin can be determined by plotting the results against their respective concentrations, as seen in Figure 4.3.

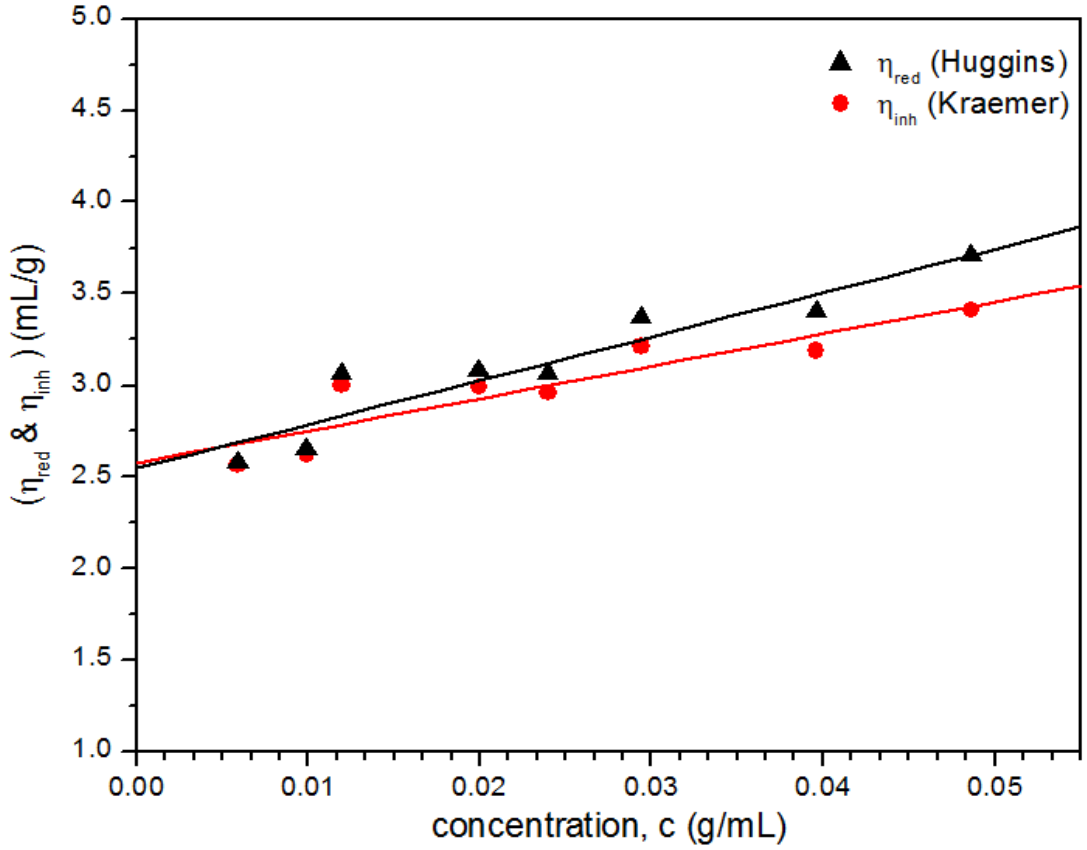

Figure 4.3: Intrinsic viscosity determination of vancomycin through the extrapolation of the reduced and inherent viscosities to zero concentration, at 20.0°C.

The plot shows the linear regression of the Huggins and Kraemer plots, both of which show a positive slope, to zero concentration. The y-intercept for both data series shows an intrinsic viscosity value of (2.6± 0.2) mL/g. With regard to both data series in the Figure 4.3, the data points at the lower concentrations (6, 10 & 12 g/mL) have a large impact on determining the final [η] value. However a limitation of this is that the impact of error, through noise, increases at these concentrations effecting the final [η]. The data points in Figure 4 for the lower concentrations do not show large degrees of variation, meaning that the resulting y-intercept of 2.6 mL/g can be taken as reliable for both data series.

The small [η] value of 2.6 mL/g for vancomycin is to be expected owing to its low molecular weight and small size. Low molecular weight globular proteins also tend to have low [η] ranging between 2.5-3.5 mL/g (Tanford, 1961).

4.3.3 Sedimentation Equilibrium

Vancomycin sedimentation equilibrium data for all dilutions of each buffer condition were analysed using SEDFIT-MSTAR. A baseline was found, data noise was removed by subtracting the average of the first 5 scans from the average of the last 5 scans (2.3.1.2), this was used to aid in determining the concentration at the meniscus for each solution. Similar to the results in 3.3.4, the baseline corrected data was used to yield plots showing; ln(c) vs r^2, M* vs r and $M_{W,app}(r)$ vs c(r) as well as the concentration as a function of fringe units against radius. Using the data from the M* and $M_{w,app}(r)$ plots the M* and hinge point molecular weights were found, Table 4.4 gives the values of both M* and hinge points determination for M_w for each solvent condition.

Table 4.4: Molar mass estimations of vancomycin in the presence of all buffer conditions, showing the M* and hinge point evaluations of M_w.

	HEPES Only		HEPES + NaCl		HEPES + NaCl + Glycerol		Water and NaCl	
conc (mg/ml)	M* (kDa)	Hinge (kDa)	M* (kDa)	Hinge (kDa)	M* (kDa)	Hinge (kDa)	M* (kDa)	Hinge (kDa)
10	2.90	2.83	3.40	3.34	3.10	3.02	3.50	3.29
5	2.70	2.62	2.70	2.54	2.60	2.64	3.00	2.86
2.5	2.70	2.85	2.70	2.64	2.80	2.76	2.80	2.68
1.25	-	-	2.50	2.46	2.10	2.08	2.20	2.20
0.6	2.10	2.15	2.50	2.51	1.90	1.90	1.60	1.62

The results of the SEDFIT-MSTAR analysis shown in Table 4.4 show that as the vancomycin concentration increases so too does the weight average molar mass.

The molecular weight of monomeric vancomycin is 1449 Da, therefore dimeric vancomycin will have a molecular weight of 2898 Da. The results in Table 4.4 show that at higher concentrations the vancomycin is in its dimeric form. This is suggested by the weight average molar mass being approximately 3000 Da. Although the higher concentrations indicate the presence of dimeric vancomycin, a degree of error is attributed to the values (±~10%). The error in these values is attributed to the optical systems, radial calibration, rotor speed and consistency calibration and temperature equilibrium of the AUC, the construction and state of the cells, as well as the concentration determination through SEDFIT-MSTAR. In addition the low molecular weight of vancomycin contributes to the error in these parameters thus leading to a ±10% error. With the error taken into account the molecular weights still indicate the presence of dimeric vancomycin.

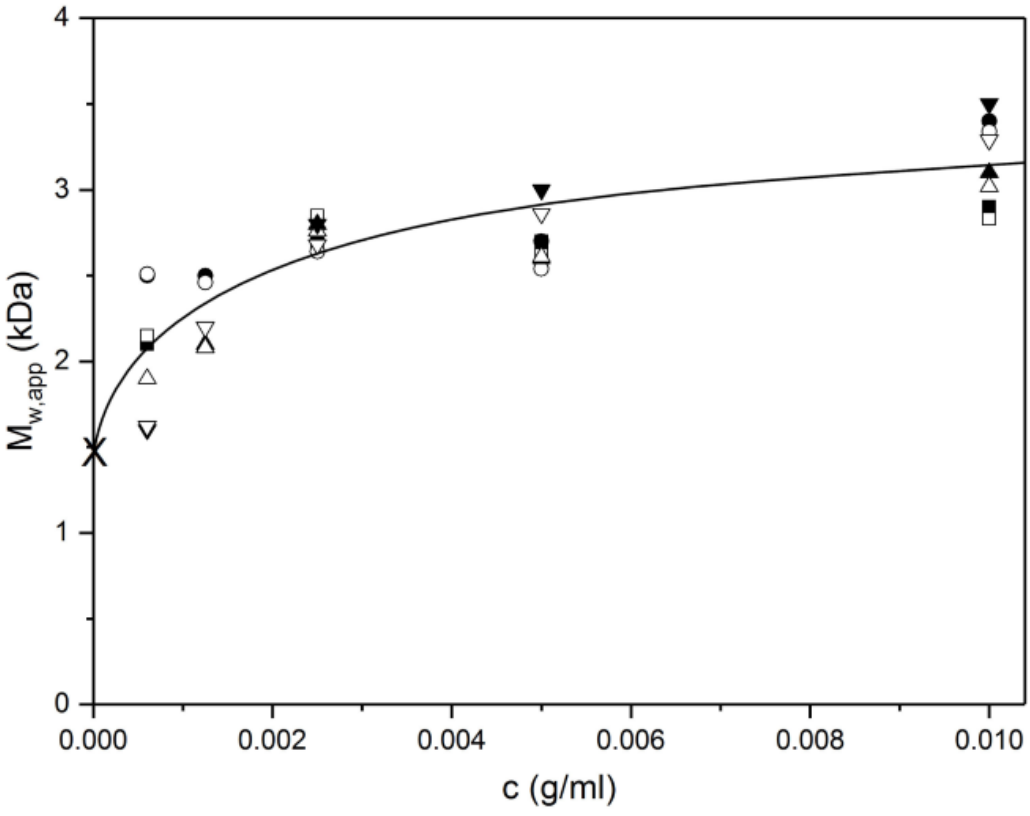

Figure 4.4: Changes of weight average molar mass of vancomycin with concentration. M* values (closed signals) and hinge point values (open symbols). Squares: HEPES alone. Circles: HEPES + NaCl. Up triangles: HEPES + NaCl + glycerol. Down triangles: Water + 0.9% NaCl.

The $M_{W,app}(r)$ vs c(r) distributions for each concentration of a given solvent, used to determine the weight average molar masses by M* and hinge point analysis shown in Figure 4.4, were combined within Figure 4.5 to give an overall concentration distribution. The plot shows the weight average molar mass of the local concentration at a given radius, c(r), for each buffer condition; (A) 100mM HEPES, (B) 100mMHEPES + 100mM NaCl, (C) 100mM HEPES + 100mM NaCl + 20% Glycerol and (D) water + 0.9% NaCl.

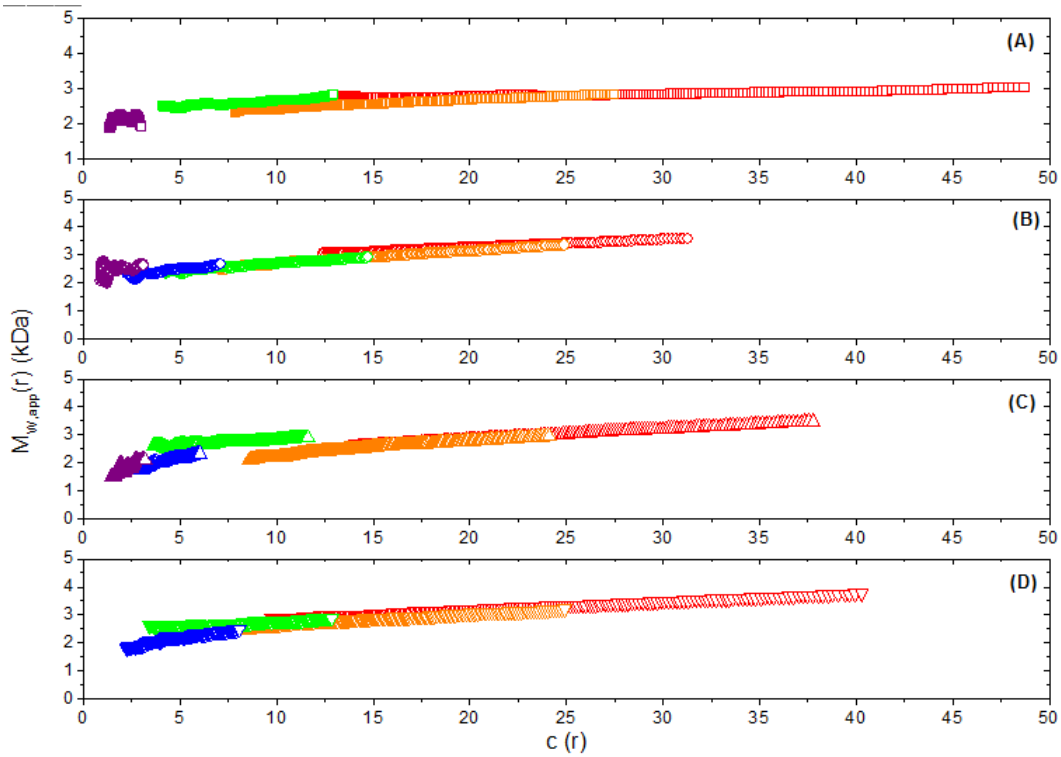

Figure 4.5: Sedimentation equilibrium plots ($M_{W,app}(r)$ vs c(r)) of each concentration (A-D) overlaid for each solvent condition. (red) 10mg/mL, (orange) 5mg/mL, (green) 2.5mg/mL, (blue) 1.25mg/mL and (purple) 0.6mg/mL.

The distributions shown in Figure 4.5 concur with the results seen in both Table 4.4 and Figure 4.4. All four plots show a molecular weight of ~1.5kDa at low concentration indicating the presence of monomeric vancomycin, however as the concentration increases the molecular weight increases and plateaus of at ~3kDa which suggests that the vancomycin is in its dimeric form. Both Figures 4.4 and 4.5 show that at a concentration of approximately 5mg/mL all of the vancomycin is in its dimeric form.

The distributions within Figure 4.5 show evidence that the dimerisation of vancomycin is reversible. A study by Roark & Yphantis (1969) showed that

sedimentation equilibrium profiles, of a given concentration range, of a fully reversible system should overlay each other. The profiles in Figure 4.5 for each buffer condition show this overlaying, thus indicating that the dimer formation of vancomycin is fully reversible. Assuming that the dimerisation is reversible both the association and dissociation constants can be determined.

4.3.4 Determining the Association and Dissociation constants

As stated above the results shown in Figure 4.5 show that the dimerisation of vancomycin is reversible. Using the data the strength of the association can be calculated using three parameters are defined; k_2 (association constant), K_2 (molar association constant) and K_d the molar dissociation constant ($1/K_2$).

Using Equation III-66 of Kim et al. (1977), shown in Equation 4.2, the Y(c) values as a function of concentration for each of the 4 solvent conditions can be determined:

$$Y(c)= \frac{M_1(M_w(c)-M_1)}{((2M_1-M_w(c))^2} = k_2.c \qquad (4.2)$$

where M_1 is the monomer molar mass of vancomycin (1449 Da) and $M_w(c)$ is the molar mass determined by SE analysis for each loading concentration, c. By subsequently plotting the Y(c) of each buffer concentration against their respective concentration, then plotting a linear line yields the k_2 value. Figure 4.6 shows the Y(c) plots for concentration 0.6, 1.25 & 2.5 mg/mL as it is at these concentrations where the vancomycin is dimerising.

Using the slope (k_2) values the K_2 values can be determined by multiplying the k_2 value by the vancomycin monomer molar mass (1449). The K_d is the inverse of this (i.e. $1/K_2$). Table 4.5 shows the values of each parameter.

Table 4. 5: k_2, K_2 & K_d values for each buffer concentration.

Solvent	k_2 (mL/g)	K_2 (M^{-1})	K_d (μM)
10mM HEPES	18400 ±2000	27600 ±3000	35 ±5
10mM HEPES + 100mM NaCl	13100 ±2000	20000 ±3000	50 ±10
10mM HEPES + 100mM NaCl + 20% Glycerol	14500 ±3000	22000 ±4000	45 ±10
0.9% (w/v) NaCl	14400 ±3000	21000 ±4000	50 ±10

From the data provided in Table 4.5 it can be seen the K_d values of each buffer condition are relatively low, ranging between 30 - 60μM. This is an indication that the dimerisation of the vancomycin monomers is relatively weak. A study by Linsdell et al., (1996) obtained a K_d value of 250μM, which although a larger value (the precise details of the evaluation method is not described) than the obtained from this investigation (hence weaker interactions) all indicates that there is a weak interaction. In addition to this both this investigation and the study by Linsdell showed a similar error of ~20% in the K_d values. As both results in each investigation support each other it can be said that the dimerisation of vancomycin is a weak interaction.

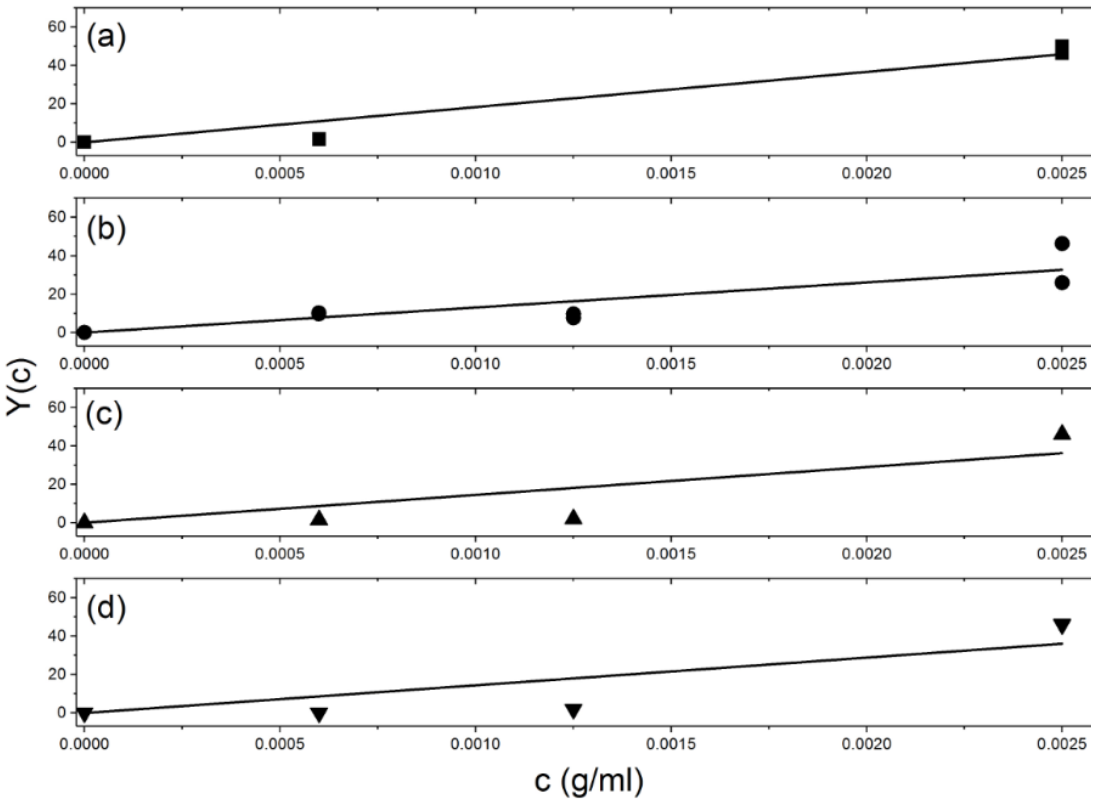

Figure 4.6: Y(c) plots of each solvent conditions at concentrations of 0.60, 1.25 & 2.50 mg/mL: (a) HEPES alone, (b) HEPES + NaCl, (c) HEPES + NaCl + glycerol, and (d) 0.9% NaCl. The slopes of each plot yield the k_2 values.

4.3.5 Vancomycin and mucin interaction SV analysis

The sedimentation velocity data of the interaction studies between vancomycin and PGM were analysed using SEDFIT. This work was done in conjunction with Hayley Coupe.

The result of the first SV runs between 12.5 mg/mL and 2.0 mg/mL PGM at 3000 rpm and 2.0 mg/mL PGM alone can be seen in Figure 4.7. The bottom distribution shows two peaks, a narrow peak at ~2S and a broader peak at ~11S after being centrifuged at 30,000 rpm. The narrow 2S peak is attributed to lower molecular weight contaminants. The main peak at ~11S is indicative of the sedimentation coefficient of PGM (Bansil & Turner, 2006). The peak is broad which reflects polydispersity within the solution due to the glycosylation of PGM.

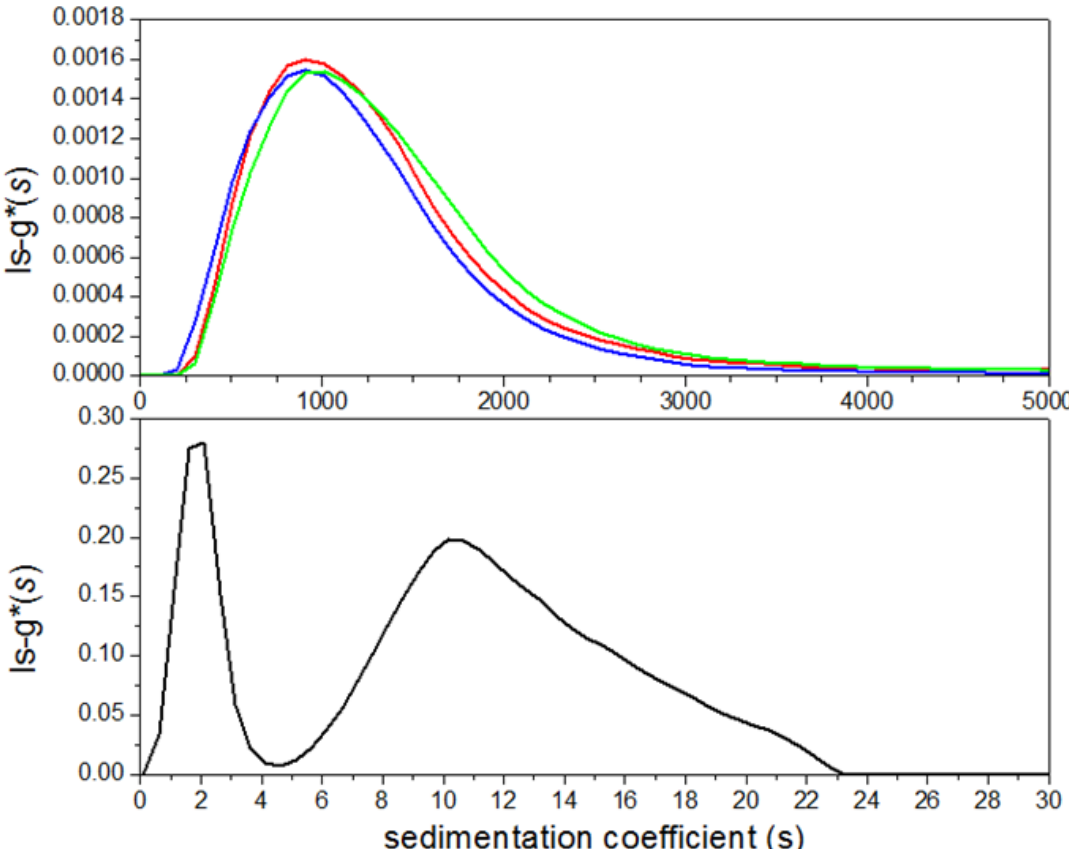

Figure 4.7: Sedimentation velocity ls-g*(s) distributions of (Top) 12.5 mg/mL vancomycin and 2.0 mg/mL PGM (x3 repeats) 3000rpm, (Bottom) 2.0 mg/mL PGM alone 30,000 rpm.

The top plot shows the distribution of the SV runs involving the mixtures of 12.5 mg/mL vancomycin and 2.0 mg/mL PGM run at 3000 rpm. The distribution indicates that the mass aggregation of the PGM has occurred as the value has increased from 11 S (monomer) to 1100 S, this suggests that vancomycin causes the mass aggregation of PGM. The results also show that aggregation occurs at a very fast rate, as using just the first 50 scans (1.5hrs) yields the same result as the use of all scans (Figure 4.7). The formation of the large PGM/vancomycin complex also explains the presence of the thick sedimented layer at the bottom of the cells.

The results of the interaction study clearly showed that vancomycin interacts with PGM and causes mass aggregation, however from this data it was unclear at what concentration vancomycin stop causing mass aggregation of PGM.

Knowing that 12.5 mg/mL vancomycin causes PGM aggregation two additional dilutions were prepared to a concentration of 1.25 mg/mL (10x)

and 0.125 mg/mL (100x), both were added to 2.0 mg/mL PGM. As before the samples were spun at 3000 rpm for 5 hours, after which the SV data was analysed in SEDFIT (Figure 4.8).

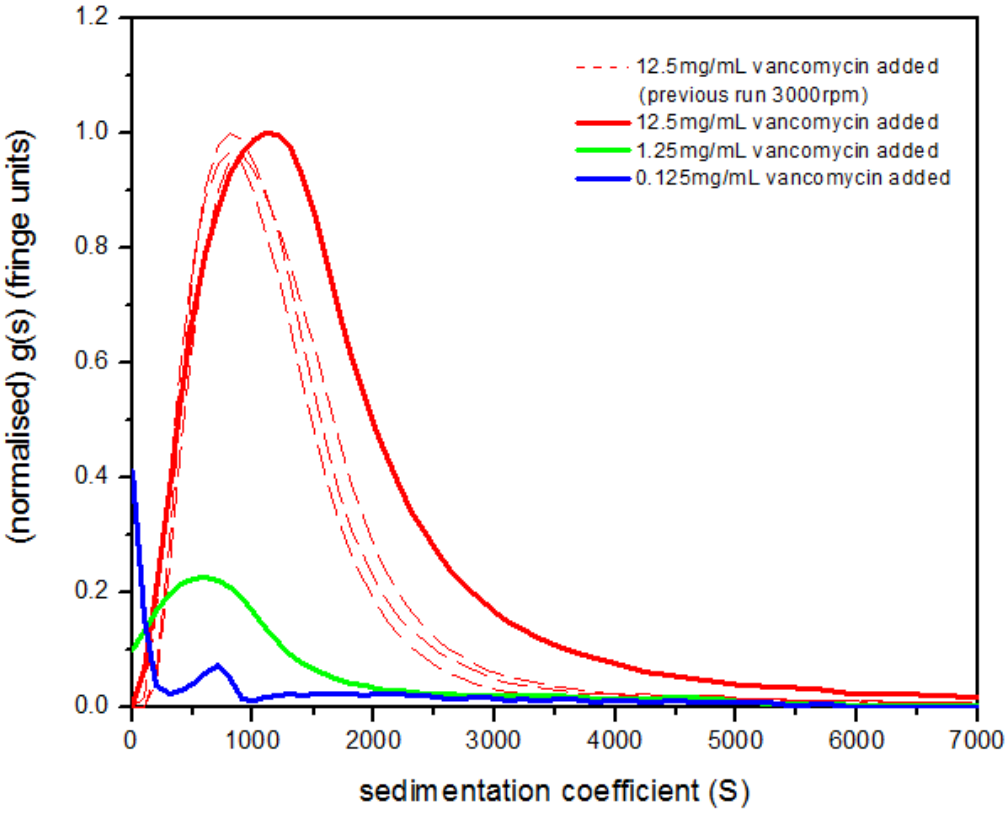

Figure 4.8: SV (3000 rpm) distribution of vancomycin + PGM at different concentrations of vancomycin (normalised); 12.5mg/mL (red) (dotted red line, previous study), 1.25 mg/mL (green) and 0.125 mg/mL (blue).

The distribution in Figure 4.8 has been normalised to the 12.5 mg/mL vancomycin run. The results clearly show that again the addition of 12.5mg/mL vancomycin causes mass aggregation of the PGM, with a complex with a sedimentation coefficient of ~1200 S forming. By integrating this data it can be seen that the peak represents ~90% of the data, indicating most of the PGM has aggregated. The first dilution of 1.25mg/mL vancomycin shows that there is a dramatic decrease in PGM aggregation, as the complex has a lower *s* ~1000 S. Again integrating the data reveals the peak represents ~50% of the data. The distribution of the 0.125 mg/mL vancomycin suggests minimal aggregation as the peak represents only ~12% of the data, suggesting an *s* of ~800S. It can

therefore be seen that as the concentration of vancomycin decreases by 10 and 100 fold there is a dramatic decrease aggregation.

In order to support the results seen in Figure 4.8 the sample was left to run in the centrifuge at an increased speed (30,000 rpm) for 12 hours, the purpose being to see if there was any non-aggregated PGM left within the cells. The results of the increased speed can be seen in Figure 4.9.

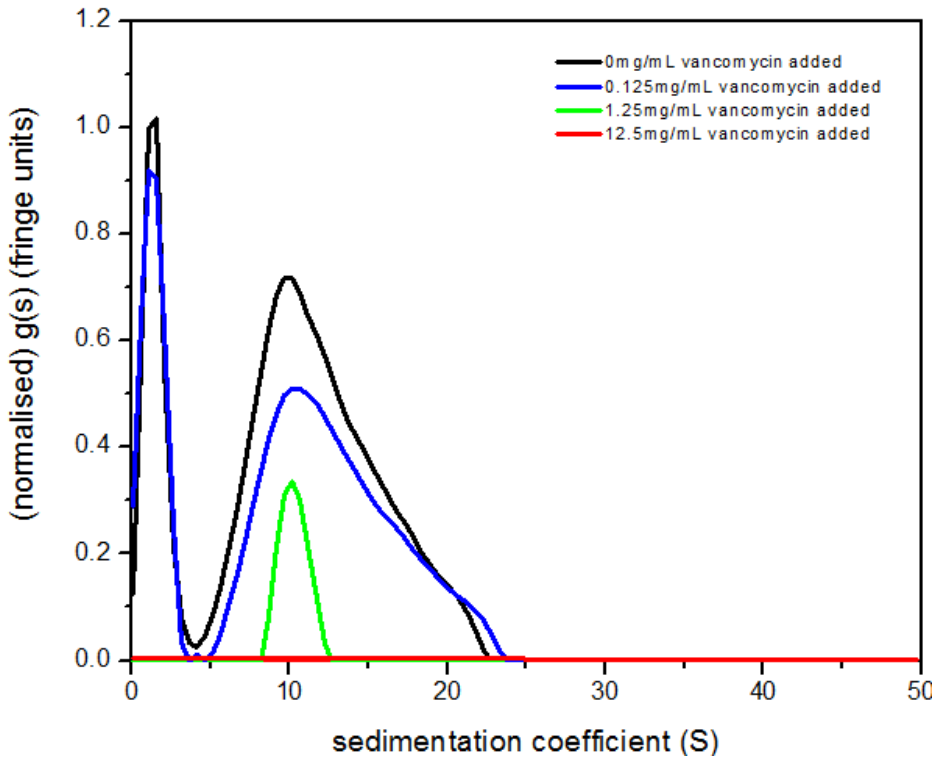

Figure 4.9: SV (30,000 rpm) distribution of vancomycin + PGM at different concentrations of vancomycin (normalised); 12.5mg/mL (red), 1.25 mg/mL (green), 0.125 mg/mL (blue) and PGM alone (black).

The distributions seen in Figure 4.9 support to a large extent the conclusions made based on Figure 4.8. From the distribution the sedimentation coefficient for PGM alone is shown to be ~11 S, this is the same value as indicated in Figure 4.7 (top). The results of the 0.125mg/mL vancomycin solution show the same at 30,000 rpm a very similar distribution is observed, this would suggest that this concentration results in little aggregation with predominantly monomeric PGM present. This is corroborated by the data in Figure 4.8, which showed that little to no PGM aggregates formed. With regard to the 1.25 mg/mL vancomycin sample

the data showed the formation of a single peak with a sedimentation coefficient of 11 S. The area under the curve in Figure 4.9 indicates that the monomeric PGM is at a much lower concentration, compared to the 0.125 mg/mL sample, this suggests that more aggregation has occurred and supports the data shown in Figure 4.8 (green). Finally the data of the 12.5 mg/mL vancomycin shows a flat indicating that no monomeric PGM is present within the cell, supporting the claim in Figure 4.8 thus indicating that all of the PGM has aggregated.

Overall the results seen in Figures 4.8 and 4.9 complement each other, the data suggests that between 0.125 mg/mL and 1.25 mg/mL vancomycin there is a critical concentration that vastly reduces the aggregation of PGM. These results are intriguing as vancomycin is orally administered four times a day at an average concentration of 125 mgs. The results of this study would suggest that at this concentration the vancomycin would cause mass aggregation of PGM, and as it is a homolog to the human gastric mucin (HGM) it can be assumed the same would occur in the human gut. Therefore it can be hypothesised that this mass aggregation, due to the high administrative concentrations, could be a large contributing factor for the poor absorption of vancomycin within the gut. It can also be suggested that the aggregates may also be the cause of indigestion, as the mucin not be properly lubricating the gut resulting in poor movement of the food within the gut.

4.3.6 Conclusion

In conclusion the hydrodynamic characterisation yielded information regarding the viscosity, dimerisation and interactions of vancomycin.
Viscometry analysis showed that the intrinsic viscosity of vancomycin was ~2.55mL/g. The low intrinsic viscosity value likely a result of the low molecular weight.

Sedimentation equilibrium analysis of vancomycin showed that in solution, and without the presence of a ligand, it forms dimers. Using M* and hinge point method evaluations for the weight average molar masses M_w and plots of the point weight average molar masses ($M_{w,app}(r)$ vs c(r)) indicate that at low concentrations vancomycin is monomeric, however as concentrations increase to above 2.5 - 5.0 mg/mL it is apparent that vancomycin is dimeric. From the SE analysis the K_d values of the dimeric vancomycin were calculated to be between 30-60 μM in all solvent condition, indicating that the dimerisation of vancomycin is relatively weak.

The interaction study between vancomycin and PGM showed that at a relatively low concentration vancomycin causes aggregation of PGM. The investigation showed that at high concentrations (12.5 mg/mL) vancomycin caused mass aggregation of PGM, with a sedimentation coefficient in excess of 1000 S. As the concentration was reduced the degree of aggregation also decreased until a concentration of 0.125mg/mL produced virtually no aggregates. The results indicate that a critical concentration between 1.250 - 0.125 mg/mL causes the formation of PGM/vancomycin aggregates.

5 Hydrodynamic characterisation of β-glucans

5.1 Introduction

β-glucans are a class of polysaccharide that are typically found in the cell walls of plant cereals, bacteria and fungi. The function of β-glucans within the cell wall are not entirely understood however recent studies have shown that β-glucans can form hydrogels within the cell wall, which may be used as a tethering point for other polysaccharides during cell growth (Kiemel et al., 2014). This investigation looks at two types of cell wall β-glucans, one sort of low molecular weight derived from a fungus (*Macrolepiota procera* (M.P)) and another of high molecualr weight from oat species. The β-glucan content between the two species differ, with oats containing approximately ~4% of the dry mass whereas mushrooms tend to contain ~8% of the dry mass (Hubner et al, (2010) & Rhee et al (2008)).

Both mushroom and oat β-glucans are of increasing importance at the moment due to recent studies showing their impact on several health conditions. Mushroom derived β-glucans have been shown to have anti-tumor properties, such as the reduction of tumours and increasing macrophage activity (Wang et al., 2005). Oat β-glucans however have been shown to reduce the levels of cholesterol within the blood, through binding to the cholesterol within the gut reducing absorption (Daou & Zhang, 2012).

Generally β-glucans have a common backbone structure composed of a linear chain of D-glucose monomers joined by β,1-3 glycosidic bonds, however between species there are difference such as additional linkages and branching (Rahar et al., 2011). The structure of β-glucans derived from fungal species predominantly have a backbone formed of β,1-3 linked glucose monomers, however there are additional β,1-6 branch points at intermittent points (Zhu et al., 2015). In comparison β-glucans derived from oat species shows a β,1-3 and β,1-4 linkages, with tri and tetra β,1-4 subunits forming linked by β,1-3 glycosidic bonds (Cui et al., 2000) . Figure 5.1 depicts the structures of the β-glucans derived from both mushroom and oat species.

β-glucans are characteristically large macromolecules with average molecular weights ranging between 20–900kDa depending on the source, with oat β-glucans having higher molecular weights (+200 kDa) than fungal β-glucans (Roubroeks et al, (2000) & Zhang et al., (2003)). The molecular weights of β-glucans can be affected by the extraction methods, as this can result in low or higher molecular weight extracts. Typically proteolytic enzymes are used to destroy hydrolytic enzymes that would degrade β-glucans within the cell wall, therefore extraction using this method often yields higher molecular weight β-glucans (Gamel et al., 2014). Although the sizes (M_w) and linkages differ between species, generally β-glucans adopt a similar structure of a random coil (Varum et al., 1991). A result of both these aspects, size and conformation, is that many β-glucans having low solubilities as well as high viscosities.

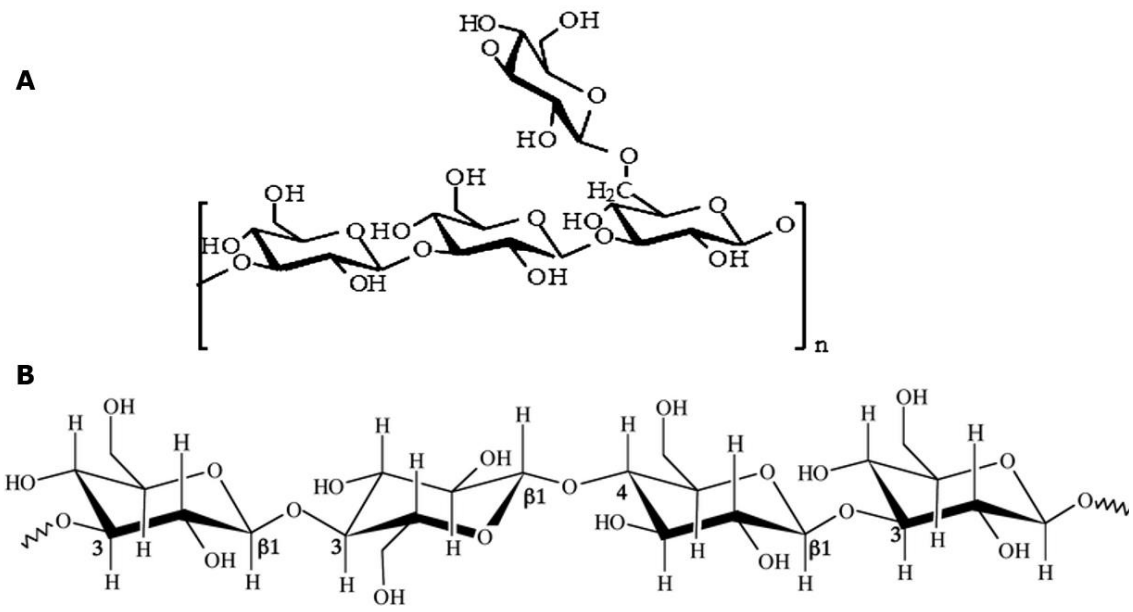

Figure 5.1: Structure of β-glucans derived from mushroom and oat species. (A) Mushroom β,1-3 backbone with β,1-6 branch point, (B) oat β,1-3 and β,1-4 linked backbone. (A) Laroche & Michaud (2007) and (B) Pillai et al. (2005).

The solubility of oat β-glucans they are dependent upon the amount of tri/tetra subunits that are present within the β-glucans. If the β-glucans consist of a similar subunit distribution then they are able to for aggregate together, thus reducing the solubility of the β-glucan, as they can for interactions between each chain. However, if there is not a consistent

subunit distribution then uniformity is vastly reduced inhibiting the formation of aggregates, thus increasing solubility (Burton et al., 2010). Generally the solubility of oat β-glucans in water is good however better with salts. The viscosity of oat β-glucans is generally very high, owing to the size and solubility. Typical viscosity values for oat β-glucans of an average molecular weight (200 kDa) are ~350 mL/g (Lazararidou et al., 2003). Measurements of viscosity are often used to indicate the molecular weight of β-glucans.

With regard to the solubility and viscosity of mushroom derived β-glucans, they are different from their oat counterparts. The solubility of mushroom β-glucans are generally poor this if often due to the structure of the molecule, however there is not a lot of evidence to show this. As seen in Figure 5.1 the β,1-3 backbone is flat linear, it has been suggested that the linear chain allows back-back interactions to form between β-glucan chains. In addition the branch points have been suggested to interact with branch chains on other β-glucans as well, resulting the formation of aggregates and thus reducing solubility (Wasser, 2011). Mushroom β-glucans are virtually insoluble in water however more soluble in alkali solution, in addition high mixing temperatures are often applied to increase solubility further (Zhu et al., 2015).
The viscosity of mushroom β-glucans is almost the polar opposite to oat β-glucans, in that these β-glucans have much lower intrinsic viscosities ranging in the 10’s not 100’s mL/g (Kimura et al., 2006).

5.1.1 Aim of investigation

The aim of the investigation is to characterise and compare the hydrodynamic properties of two different β-glucans obtained from mushroom and oat sources. The hydrodynamic characterisation involves:

- Viscosity measurements to determine if there is a considerable difference between each species.
- SV analysis to determine the sedimentation coefficient and heterogeneity of each β-glucan type.
- SE analysis to estimate the weight average molar mass of the β-glucan samples.

5.2 Materials and Methods

5.2.1 Materials

A 1L phosphate buffered saline (PBS) solution of pH 7.0 was prepared using 2.923g sodium chloride, 1.561g dihydrogen potassium orthophosphate and 4.595g sodium dihydrogen dodecahydrate, obtained from Sigma Aldrich, UK. A 2L 0.1M sodium nitrate ($NaNO_3$) (Sigma Aldrich, UK) dialysis solution was produced.

Two β-glucans were provided from different sources. The first β-glucan were derived from an unknown oat species provided by NOFIMA (Norway), they consisted of six samples (7-12) of the same β-glucan. The second β-glucan can from the mushroom species *Macrolepiota procera* (M.P), the sample was provided by Dr Cleanthes Israilides, NAGREF, Lykovrysi, Greece.

5.2.2 Mushroom (M.P) β-glucan sample preparation

From the powdered sample of the M.P β-glucan a stock solution was prepared to a nominal concentration of 7.0 mg/mL in 40mL PBS buffer. Owing to the high difficulty of getting β-glucans into solution (Zhu et al., 2015), the solution was heated to 90°C and left on a gentle stir for 5 hours. A large majority of the β-glucan was in solution however not fully, in order to remove the insoluble β-glucan material the sample was centrifuged at 2000 rpm for five minutes to remove the large insoluble material. After centrifugation the supernatant was removed with the pellet placed into the fridge.

The concentration of the supernatant was determined using the refractometer, with a dn/dc value of 0.146 mL/g (Li et al., 2006), this was revealed to be 6.4 mg/mL. Using the supernatant stock solution a dilution series was produced consisting of 5.0, 4.0, 3.0, 1.0, 0.5 and 0.3mg/mL β-glucan in PBS.

5.2.3 Oat β-glucan sample preparation

The samples of β-glucans from NOFIMA were supplied by Dr. S. Ballance in a solution of water with 0.02% sodium azide. The samples were said to contain possible low molecular weight contaminants, therefore the samples were dialysed. Dialysis was carried by placing 100mL of each β-glucan sample into a 40mm wide cellulose based dialysis tubing, with a molecular weight cut off of 12-14kDa. The samples were placed into 1L of $NaNO_3$ and left for 6 hours after which the dialysed $NaNO_3$ (dialysate) was removed and kept, an additional 1L of $NaNO_3$ was added to the sample and left overnight. Once dialysis was complete the dialysate was removed and placed with the previous dialysate. The samples were removed from the dialysis tubing and placed into containers.

Concentration estimates of the samples were provided by NOFIMA, obtained from enzymatic digestion of the β-glucans. However due to the dialysis the concentrations were determined again using the refractometer. The measurements were carried out as in 2.2.2, using a dn/dc value of 0.146 mL/g (Li et al., 2006). The results from the refractometery were placed in Table 5.1 along with the enzyme digestion concentrations.

5.2.4 Density and Viscosity measurements

The density measurements for both β-glucan species were conducted in the same manner, using the method outlined in 2.1.2 with the Anton Paar DMA5000 density meter. Density measurements for the mushroom β-glucan samples were carried out on the higher concentration solutions, leaving out the 1.0, 0.5 & 0.3 mg/mL dilutions. The individual samples of oat β-glucan from NOFIMA were measured using the same method.

Viscosity measurements were conducted using the method outlined in 2.1.4, using an Ostwald U-tube viscometer and the Schott-Geräte AVS 400 timing unit, recording the flow times. The flow time's mushroom β-glucan samples were recorded at a temperature of 20.0°C. Likewise the same procedure was carried out for the oat β-glucan samples. The results were recorded in Table 5.2 along with the subsequent calculated viscosities.

5.2.5 Mushroom and Oat β-glucan SV analysis

SV analysis was carried out using the Beckman XLI-AUC, using 12mm aluminium cases containing an epoxy centrepiece. Data analysis of the scans was carried out using SEDFIT producing both ls-g*(*s*) and c(*s*) distributions (refer to 2.3.1.1).

Mushroom β-glucans

The low concentration β-glucan samples of 1.0, 0.5 & 0.3mg/mL were analysed. Each concentration was inserted into one of three cells to a volume of 0.4mL, along with 0.4mL of the PBS buffer in the other corresponding sector. The cells were inserted into the 4 hole Ti rotor and placed into the AUC chamber set at 20.0°C. A rotor speed of 3000 rpm was applied to adjust the fringes, after which a speed of 50,000 rpm was used, with measurements made using Rayleigh interference optics. Scans were taken at 2 minute intervals until 500 scans were acquired.
For analysis on SEDFIT a solvent density and $\bar{v}$ of 1.0032 g/mL (measured by density meter) and 0.60 mL/g (Woodward et al., 1983) were used, respectfully.

Oat β-glucans

Each sample was loaded into one of six cells to a volume of 0.4mL with 0.4mL of the dialysate buffer injected into the adjacent corresponding sector, a cell containing just water was also prepared. The cells were placed into the 8 hole Ti rotor and placed into the AUC, set at 20.0°C. A speed of 3000 rpm was applied to optimise the fringes, upon which a speed of 45,000 rpm was applied. Measurements were made using Rayleigh interference optics at 2 minute intervals until a total of 500 scans were acquired. For SEDFIT a $\bar{v}$ of 0.6 mL/g and solvent density of 1.0039 g/mL were used.

5.2.6 Mushroom and Oat β-glucan SE analysis

SE was carried out using the Beckman XLI-AUC, using the 20mm titanium centrepieces in aluminium cases. All SE data was analysed using SEDFIT-MSTAR using the average of the last 5 scans minus the average of first 5 scans (refer to 2.3.1.2). The parameters used in the SV analysis for both β-glucans were used again for SE analysis.

Mushroom β-glucan

The same three samples used in the SV analysis were used again. Of each sample 0.15mL was inserted into one of three cells, in addition 0.15mL of PBS buffer was injected into the adjacent sector. The samples were placed into the 4 hole Ti role and placed into the AUC, set at 20.0°C. The fringes were adjusted at 3000 rpm, with the speed increased 30,000 rpm thereafter. The samples were centrifuged for 72 hours, with measurements made using Rayleigh interference optics every 1 hour. Five scans were taken at the beginning and end of the run in addition.

Oat β-glucan

SE analysis of the NOFIMA β-glucans was carried out using the same six samples in the SV analysis. A sample volume of 0.15mL was inserted into each cell along with an equal volume of the dialysate buffer. The cells were loaded into a 8 hole Ti rotor and placed into the AUC, set at 20.0°C. A rotor speed of 3000 rpm was applied to adjust the fringes. Using estimated molecular weight from the SV analysis a rotor speed of 8000 rpm was selected to be applied to the samples. Measurements were made using Rayleigh interference optics, taking readings every 1 hour for 85 hours. Five scans were taken at the beginning and end of the run in addition.

5.3 Results and Discussion

5.3.1 Mushroom β-glucan

5.3.1.1 Mushroom β-glucan viscosity

The flow times of the β-glucan concentrations, along with the density measurements, were used to determine the η_{red} and η_{inh} viscosities. Because of the low flow time increments compared to the solvent only the Solomon-Ciuta equation was applied at a single concentration, rather than a concentration extrapolation.

Table 5.1: Relative, reduced, inherent viscosities and intrinsic viscosity of M.P mushroom β-glucans (20.0°C).

Concentration (g/mL)	η_r (mL/g)	η_{red} (mL/g)	η_{inh} (mL/g)	$[\eta]$ (mL/g)
0.0064	1.022	3.424	3.387	3.413
0.0050	1.016	3.176	3.152	3.183
0.0040	1.012	2.938	2.921	2.988
0.0030	1.009	2.823	2.811	2.991

A study by Kimura et al. (2006) on β-glucans derived from a yeast like fungus (*Aureobasidium pullulans*), showed that the β,1-3 (β,1-6 branched) linked β-glucans had a low intrinsic viscosity value and molecular weight (less than 100kDa). The results of the intrinsic viscosity measurements of this investigation suggest that a similar structured β-glucan is present within the M.P mushroom species. SE analysis examined later also supports this claim.

5.3.1.2 Mushroom β-glucan SV and SE analysis

The SV data for the M.P β-glucans was analysed using SEDFIT, in each concentration every second scan of the first 250 scans was analysed. The data was used to produce both g(*s*) and c(*s*) distributions for each species. The SE data analysis involved SEDFIT-MSTAR and the method outlined in 2.3.1.2.

5.3.1.2.1 SV analysis

The SV results were used to produce a distribution plot, Figure 5.2, which shows the sedimentation coefficient of the M.P β-glucans derived from SEDFIT. Figure 5.2 shows two plots; (top) ls-g*(*s*) analysis and (bottom) c(*s*) analysis.

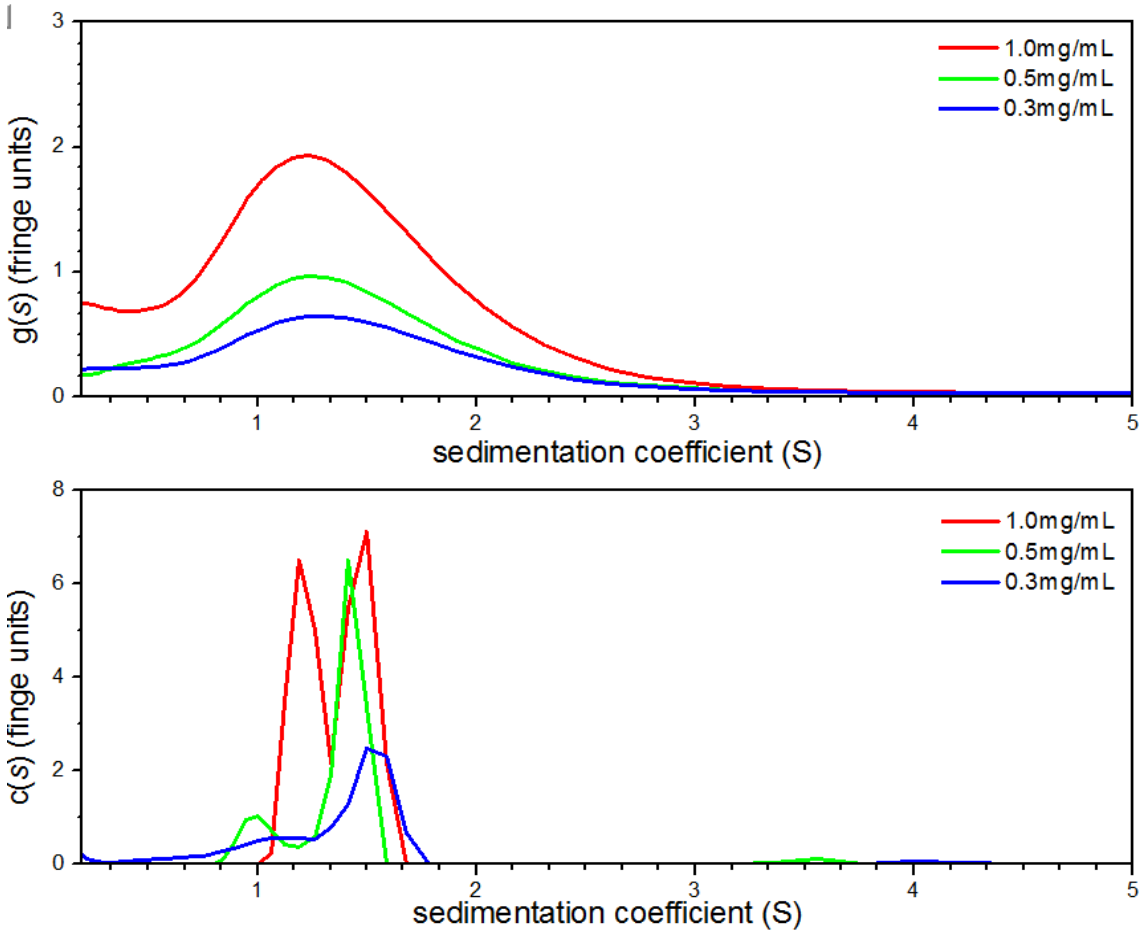

Figure 5.2: SEDFIT SV analysis of M.P β-glucan concentration series, at a rotor speed of 50,000rpm. (Top) ls-g*(s) plot and (Bottom) c(s) analysis.

The g(*s*) distribution (top) indicates that the sedimentation coefficient of the β-glucans is approximately 1.4 S, through the integration of the data peaks within SEDFIT the same sedimentation coefficients were obtained. The results are intriguing as generally as concentration reduces the sedimentation coefficient increases, due to the reduction of non-ideality. The *s* values of M.P β-glucans do not show this trend instead showing very similar *s* values as the concentration decreases. In addition the data that produces the sedimentation peaks of each concentration constitutes approximately 85% of the total signal obtained from the cell, this leads to a suggestions that the β-glucans are relatively monodispersed.

The c(*s*) plots (bottom) show a similar distribution, however characteristically of c(*s*) analysis there is an over sharpening of the peaks. This over sharpening has resulted in the formation of 2 peaks from the 1 peak seen in the g(*s*) analysis, and in addition has formed some higher sedimentation coefficient peaks. The presence of two peaks, in close proximity to each other, would suggest that there is actually only one peak present.

The low *s* values indicate that the β-glucans have a low molecular weight, using the c(M) algorithm within SEDFIT an estimated molecular weight of ~10kDa was obtained for each sample. The indication of the same molecular weight in each concentration supports the assumption made from the g(*s*) plots that the samples are relatively monodispersed.

5.3.1.2.2 SE analysis

SE analysis carried out by SEDFIT-MSTAR, yielded results for each M.P β-glucan concentration. From the data four plots were found for each concentration; c(r) vs r, lnc(r) vs r^2, M* vs r and $M_{w,app}$ c(r) vs c(r). Figure 5.3 shows the four distributions the 0.5mg/mL β-glucan, similar plots were produced for all concentrations. Using the data from SEDFIT-MSTAR for each cell the Mw determined from the M* and hinge point analysis methods, along with the polydispersity were recorded in Table 5.4.

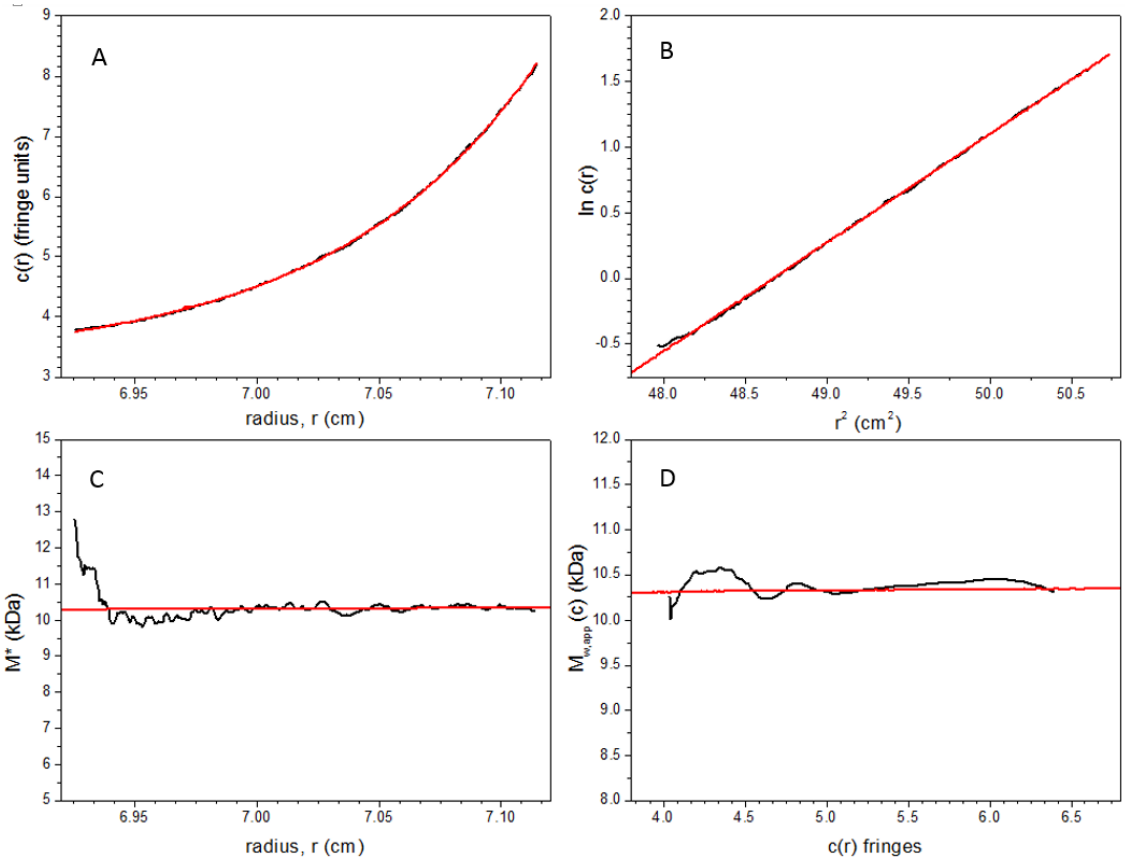

Figure 5.3: Molar mass analysis for 0.5mg/mL M.P β-glucan from SEDFIT-MSTAR: (A) Distribution of data along the radius of the cell, (B) log of concentration in the cell vs the square of the radial displacement, (C) M* analysis vs radius, (D) point average molecular weight.

Using Figure 5.3, plot (B) shows the natural logarithm of the data against the square of the radius. From the plot it can be seen that the fitted data (red) overlays the raw data (black). The overlaying of both data sets, coupled with the lack of upwards or downwards bending of the data, suggests that there is little polydispersity within the cell. Table 5.2 shows

that similar data was obtained for all the concentrations, using the M_z data the polydispersity indexes of each concentration were ~1.0. The low polydispersity index values indicate that the M.P β-glucan samples are predominantly monodispersed, thus supporting the observations from the SV distributions.

Plot (C) shows the M* analysis, this yields (from M*(r) extrapolated to the cell base) the weight average molar mass over the whole distribution, M_w. The data shows that the average molar mass, for this given concentration, is approximately 10.2 kDa. Similar M* derived molecular weights M_w were obtained for the other concentrations, Table 5.2. Plot (D) shows the local point average molecular weights $M_w(r)$ plotted against loading concentration in the ultracentrifuge cell, c(r), the distribution supports the molecular weight determined from the M* analysis indicating a molecular weight of ~10.3 kDa.

Table 5.2: Summary of weight averages of M.P β-glucans using M* and hinge point analysis, along with the polydispersity of the samples.

Sample (mg/mL)	0.3	0.5	1.0
M_w (kDa) from M*	10.0	10.1	10.3
M_w (kDa) from hinge point	10.1	10.2	10.3
M_z	10.1	10.1	10.4
Polydispersity	1.0	1.0	1.0

5.3.1.3 Shape estimation

A study by Stahmann et al (1995) regarding single stranded β-glucans with β, 1-3, β,1-6 branches have been shown to have a persistence length of 300nm. The persistence length is a measure of how rigid a molecule is, the greater the value the more rigid a molecule is. Therefore assuming the M.P β-glucans are similar in structure they will also have a high rigidity, particularly as they are low molecular weight short-chain structures, which tend to have limited flexibility compared to larger linear structures in any case. Using this information and subsequent data from the SE run an estimation of the shape of the M.P β-glucans can be made based on ellipsoidal modelling. Using SEDFIT an estimation as to the frictional ratio of the β-glucans was shown to be ~1.8 in all three concentrations. Using this value along with the *s* (1.4S), $\bar{v}$ (0.60 mL/g), molecular weight (10kDa) and an array of hydration values the Perrin function can be calculated, using BIOMOLS2. Using different hydration values; 0, 0.3, 1.0 & 2.0g g^{-1}, several Perrin function values were calculated. By using these Perrin values and inserting them into ELLIPS1 algorithm of Harding et al (2005), an estimation as to the shape of the mushroom β-glucans was made (Figure 5.4).

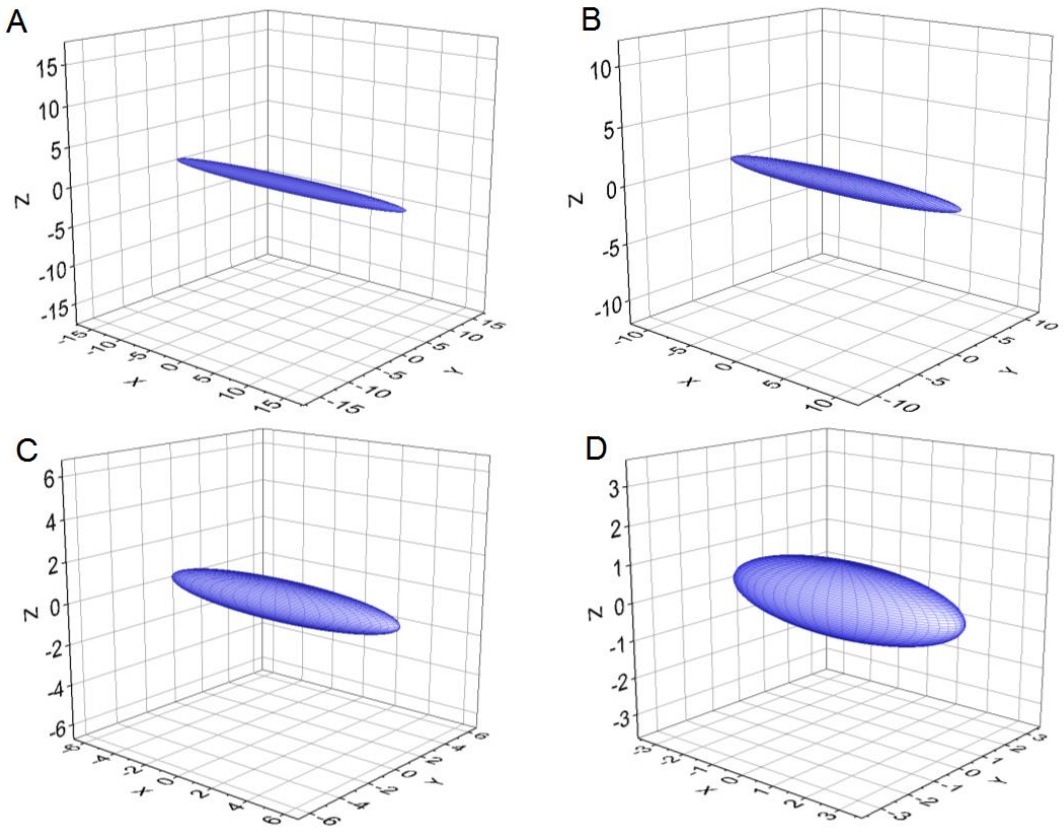

Figure 5.4: Prolate models of M.P β-glucans using different hydrations; (A) 0.0, (B) 0.3, (C) 1.0 & (D) 2.0 g water/ g of β-glucan.

β-glucans have varying degrees of hydration, therefore use a range of values it is possible to see the range of possible conformations that the β-glucans may take on. As can be seen in all plots in Figure 5.4 the shapes indicate an extended prolate with axial ratios of; (A) 4:1, (B) 7:1, (C) 13:1 and (D) 18:1. The lower hydration values are unlikely to be correct as polysaccharides often have a hydration greater than 1, therefore the latter shapes (C) and (D) are more likely to be representative of the true conformation, extended prolates.

5.3.2 Oat β-glucan

5.3.2.1 Concentration determination

After dialysing the samples overnight in $NaNO_3$ the concentration of the resulting solutions was determined using the refractometer, the results are seen in Table 5.3. The concentrations were calculated using Equation (2.11), with a dn/dc value of 0.146 mL/g (Li et al., 2006) was used for the β-glucans.

Table 5.3: M.P β-glucan concentration comparison between enzyme digestion and refractometry determination (after dialysis).

Sample	Enzyme digestion concentration (mg/mL)	Dialysed concentration (Refractometry) (mg/mL)
7	1.03	1.47
8	1.20	1.47
9	1.15	1.45
10	1.02	1.41
11	1.24	1.45
12	1.21	1.43

The results show that the original concentrations, determined by enzyme digestion, are similar to the concentrations determined (after dialysis) by refractometry. For the purpose of this study the concentrations determined using the refractometer were used. These values were chosen over the enzyme digestion as this method is more reliable due to the possible changes in concentration after dialysis.

5.3.2.2 Viscosity measurements

Viscosity measurements were carried out to ultimately estimate the size of the β-glucans.

The flow times of the oat β-glucan samples were vastly different from the mushroom β-glucans, the flow times ranged between 150 – 520 seconds. The reduced and inherent viscosities, determined from the flow times Table 5.4, indicate that the size and shape of the β-glucans are large and varied between each sample. Although the different viscosities show a wide range the Solomon-Ciuta values (an average) indicate that the bulk of the viscosities lie within the range of 400 – 1000 mL/g, with sample 9 showing a value that is much higher (1600 mL/g). Figure 5.5 shows the results of all three viscosities of each sample.

Table 5.4: Reduced and inherent viscosities of all six oat β-glucan samples, along with the Solomon-Ciuta intrinsic viscosity values (Temp= 20.0°C).

Sample	η_{red} (mL/g)	η_{inh} (mL/g)	Solomon-Ciuta [η] (mL/g)
7	590	425	474
8	852	552	638
9	3020	1160	1601
10	1241	717	862
11	904	578	671
12	1872	911	1160

Although the samples yielded a range values they all indicate that the oat β-glucans have high intrinsic viscosities. Previous studies by Doublier et al. (1995) and Lazararidou et al. (2003) showed that a preparation of an oat β-glucan with an M_w of 250 kDa had an [η] of 383.0 mL/g. Using this as a platform, and the viscosities obtained from this investigation, it can be assumed that the samples also have high molecular weights. However the use of single concentration data points does not give a true representation of the actual intrinsic viscosities of the β-glucans, this is due to effects such as non-ideality being high. Owing to time constraints further analysis was not carried out on the viscosities. Further analysis using different concentrations will allow an extrapolation of zero concentration, yielding what is likely to be a lower intrinsic viscosity for each sample.

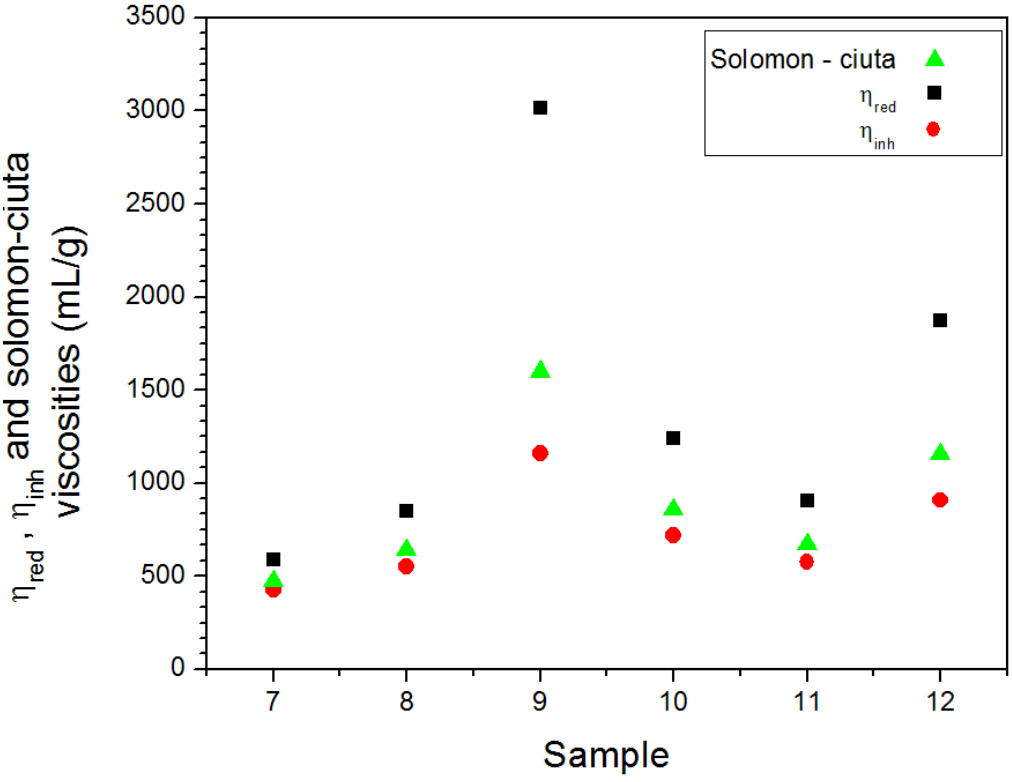

Figure 5.5: η_{red} (black) and η_{inh} (red) data points of a single concentration of each oat β-glucan sample, with the resulting Solomon-Ciuta (green) values. The data points show the majority of values lie in range of 450 – 1000 mL/g.

In addition the viscosity measurements, are immensely larger than the viscosity measurements obtained for the M.P β-glucans. This is to be expected as previous studies suggests oat β-glucans have a much larger viscosity (Lazararidou et al., 2003).

5.3.2.3 Oat β-glucan SV and SE analysis

5.3.2.3.1 SV analysis

The results of the viscosity measurements, Table 5.4, suggest that the size of the β-glucans is relatively large. Therefore it was expected that the sedimentation coefficients of the β-glucans would also be large. Using SEDFIT the SV data was analysed, producing both a g(*s*) and c(*s*) distributions seen in Figure 5.6.

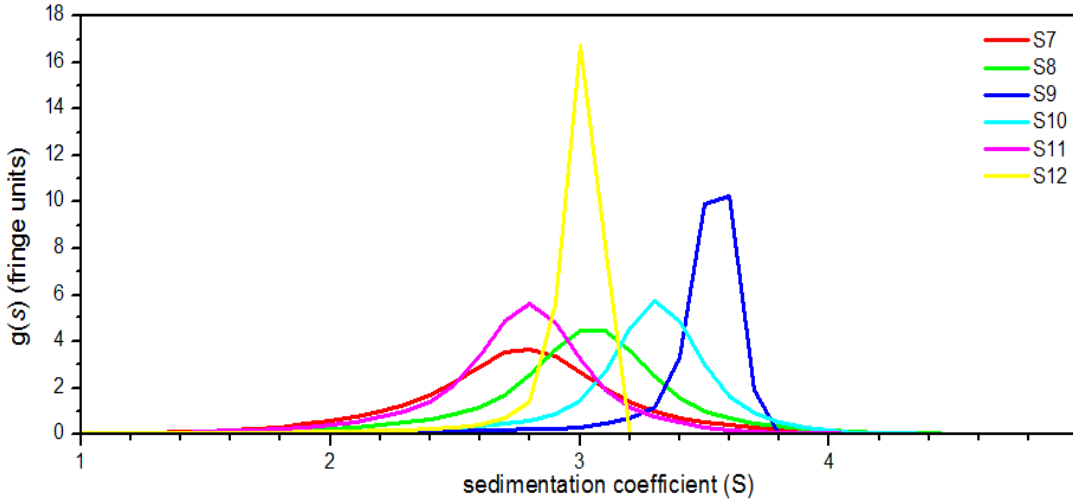

Figure 5.6: Sedimentation velocity ls-g*(s) analysis of all six NOFIMA β-glucan samples (S7-S12), at a rotor speed of 45,000rpm.

The distributions show that the sedimentation coefficients are not the same for each sample, however using the g(*s*) distribution the *s* values all lie within a range of 2.6–3.6 S.

The g(*s*) analysis shows that a single peak for each sample is present, which is an indication of a unimodal system similar to the results of the M.P β-glucans. However the broadness of the peaks suggest very high

polydispersity. A study by Woodward et al. (1983) showed that β,1-3 & β,1-4 linked β-glucans with molecular weights of 160 & 290 kDa had sedimentation coefficients of 3.5 & 4.5 S, respectively. The sedimentation values in that study are similar to the values obtained by this investigation, suggesting that the molecular weights of the oat β-glucans are approximately ~200 kDa. In order to confirm this hypothesis the use of SE data is required.

5.3.2.3.2 SE analysis

SE analysis of the oat β-glucans was carried out using SEDFIT-MSTAR, in which a baseline and loading concentration at the meniscus was determined for each sample. The analysis of the data produced four plots; c(r) vs r, lnc(r) vs r^2, M* vs r and $M_{w,app}(r)$ vs c(r). Figure 5.7 shows the four plots for Sample 7 (1.47 mg/mL).

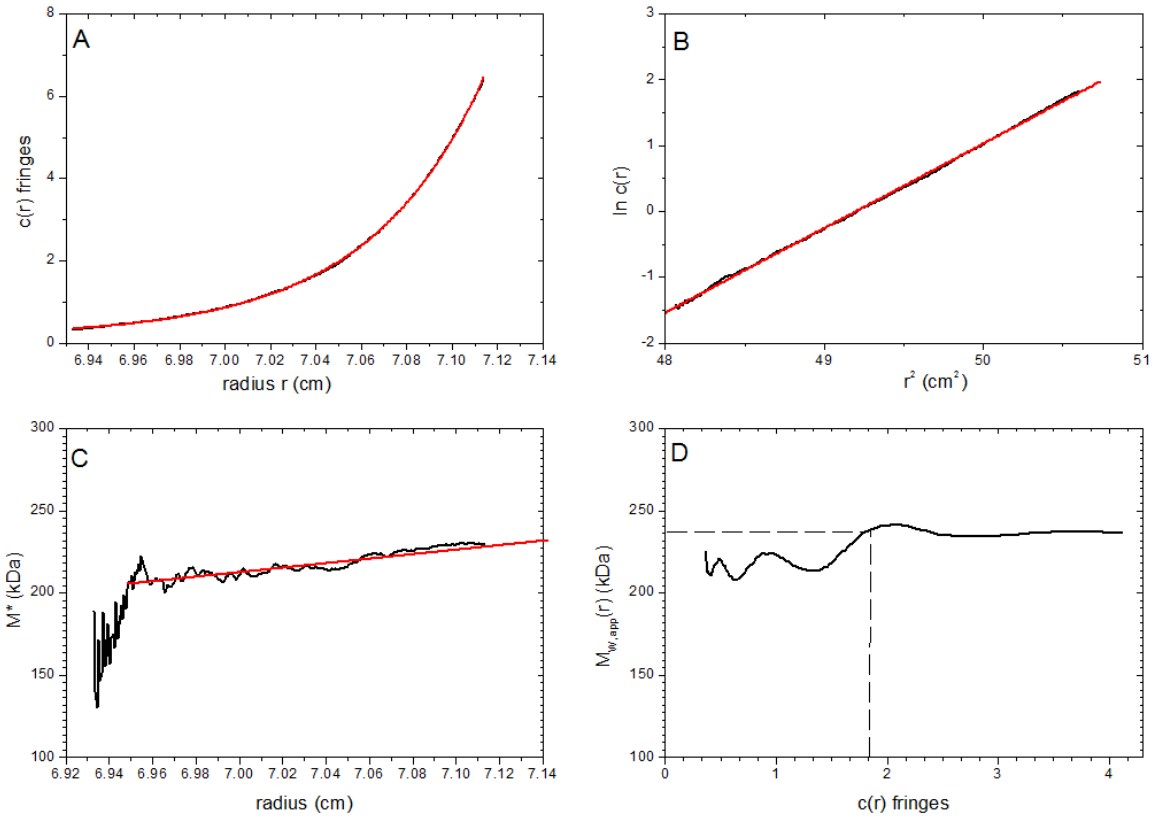

Figure 5.7: Molar mass analysis of oat β-glucan Sample 7 (1.5 mg/mL). (A) c(r) vs r, (B) lnc(r) vs r^2, (C) M* vs r & (D) $M_{w,app(}r)$ vs c(r). Hinge point Mw is shown with dotted line.

Because of the relatively high concentrations used (1.5 mg/mL), all the values are only apparent values $M_{w,app}$, i.e. not corrected for non-ideality. These will differ from the true values which would normally be determined by extrapolating $1/M_{w\ app}$ vs c to zero concentration (see Harding, 2005). This was outside the scope of this MRes study and is the subject of further research. Nonetheless $M_{w,app}$ values are shown for each sample for comparison purposes.

Table 5.5: The results of all six samples with M* and hinge point molecular weight estimations for all $M_{w,app}$, along with the respective polydispersity indices. Shown also is their respective *s* and Solomon-Ciuta [η] values.

Sample	*s,* (S)	$M_{w,app}$ from M* analysis (kDa)	$M_{w,app}$ from hinge point (kDa)	[η] (mL/g)
7	2.7	230	240	470
8	3.0	350	360	640
9	3.5	600	700	1600
10	3.3	320	330	860
11	2.8	310	320	670
12	3.0	420	400	1160

These values are all apparent values obtained at a concentration of 1.5mg/mL, and are included only for comparative purposes. Full extrapolations to zero concentration to correct for non-ideality is the subject to Further Work, beyond the scope of this MRes.

5.4 Conclusion

The investigation found that mushroom β-glucans derived from *Macrolepiota procera* were very low molecular weight with very low intrinsic viscosities. The viscosities were indicative of a small macromolecule that had both a low molecular weight and a compact structure.

The results of the SV analysis showed a molecule that had a low sedimentation coefficient (~1.4S), again indicating a small size with a low molecular weight. In corroboration with these results, regarding the small size, was the SE analysis which indicated a molecular weight for the mushroom β-glucans of approximately 10kDa. Using both the viscosities and *s* values the conformations of the β-glucans were determined.

The hydrodynamic characterisation of the oat β-glucans showed that these molecules were very different. The viscosity measurements showed that the oat β-glucans had extremely high viscosities, ranging between 400-1000mL/g, vastly different from the mushroom β-glucans. The viscosities also indicated that the molecular weight and size of these β-glucans was much larger than the mushroom β-glucans.

SV analysis showed that the oat β-glucans had a range of sedimentation coefficients (2.6-3.6S). These values were considerably larger than the mushroom β-glucans again indicating a higher molecular weight. Because of the time restrictions on the MRes, only the apparent molecular weights at a concentration of 1.5 mg/mL have been shown for comparative purposes. Nonetheless they show that oat β-glucans are much larger than they mushroom ones.

6 Concluding Remarks

6.1 Ovalbumin

The main aim of this part of the investigation was to learn and execute several hydrodynamic characterisation methods, including viscometry, density measurements and Analytical Ultracentrifuge techniques. The work carried out on ovalbumin, a previously well hydrodynamically characterised glycoprotein, allowed these techniques to be established.

Sedimentation velocity analysis showed that the ovalbumin contained significant amounts of lower molecular weight and higher molecular materials, although the main component with a sedimentation coefficient ($s_{20,w}$) value of 3.2S was present with a similar *s* to previously published values. However, both the ls-g*(*s*) and c(*s*) distributions showed the presence of lower and higher molecular weight contaminants. Even though the presence of contaminants were confirmed by SV analysis, the weight average molar mass indicated from SE was the same as the actual value of 45kDa.

Overall the intrinsic viscosity value of ovalbumin for this preparation was slightly higher than previous published values for monodispersed ovalbumin solutions, but this is consistent with what we see from sedimentation velocity analysis. This is also reflected in the slightly more elongated prediction for the shape of the molecule from ELLIPS1.

6.2 Vancomycin

The investigation into vancomycin had two main aims; determine the possible dimerisation in the absence of a ligand and determine the subsequent K_d value, and to investigate the interactions between vancomycin and gastric mucin (PGM). The investigation used methods including viscometry, SV and SE.

The first part of this investigation yielded information regarding the intrinsic viscosity of vancomycin, which was found to be ~2.55 mL/g. this value indicates a macromolecule with a small size, which is what vancomycin is (Mw 1449 Da).
The main results of the investigation found that between and above a concentration range of 2.5 - 5.0 mg/mL vancomycin forms dimers, below this range and vancomycin is predominantly monomeric. The investigation found that the dimerisation is fully reversible, with subsequent K_d values ranging between 30 - 60μM in all buffer conditions.

The second part of the investigation found that vancomycin causes mass aggregation of PGM above a concentration of 1.25 mg/mL. The results suggest that above this concentration vancomycin causes over 50% of a given PGM to aggregate, with almost all PGM forming aggregates at a concentration of 12.5 mg/mL. The results of the investigation suggest that the aggregates may be the reason for the poor absorption of vancomycin within the gut, therefore future work into this is needed to evaluate this conclusion.

6.2.1 Future work

The investigation into vancomycin yielded several important conclusion, the greatest being the aggregation of mucin through the addition of vancomycin.
An immediate continuation of the investigation will be determine what the critical concentration of vancomycin is that causes significant aggregation of PGM. In addition to this is to see of these effects are observed in other buffers.

In conjunction to the use of AUC (SV) is the possible use of a disc centrifuge (CPS), which can also be used to determine the interaction between PGM and vancomycin. CPS will also yield information regarding the macromolecular radii of the aggregates which can be used to better understand the structure of the complex that forms. This would complement the data obtained from the SV analysis.
An important continuation of this work would be to see if these effects are seen in other mucins, e.g. bovine submaxillary mucin (BSM) and human gastric mucin (HGM). The aim would be to replicate the results seen with PGM and vancomycin, thus supporting the conclusion made from this investigation.

Using the findings of this investigation and future investigations using HGM, would be to investigate the binding mechanism between vancomycin and mucin using vancomycin analogues. The use of analogues allows different areas of the vancomycin molecule to be modified, interactions studies would then determine if the modifications are detrimental to the formation of aggregates. Thus meaning that area is important in the binding between mucin and vancomycin. If the binding area is identified it would allow potent vancomycin analogues to be designed that reduces mucin aggregation and increase absorption within the GI tract.

In addition to the use of vancomycin analogues to identify the binding mechanism, is an investigation into the use of both positively and negatively charged polysaccharides as a drug delivery mechanism. A possible investigation could look at the interaction between vancomycin and chitosan (positively charged polysaccharide), as chitosan has been shown to interact with mucin (Deacon et al., 2000). If chitosan could be used to transport vancomycin then it may reduce the formation of vancomycin induced aggregates, this may lead to an increased absorption of vancomycin.

6.3 Mushroom and oat β-glucan

The investigation in both mushroom and oat β-glucans showed that there were considerable differences. Using an array of methods involving viscometry, SV, SE and shape determinations, these differences were confirmed.

The investigation showed that mushroom β-glucans have a low intrinsic viscosity. Although the actual value obtained from this investigation was not obtained, the results suggested that the β-glucans have a low viscosity and a resulting molecular weight.
The SV and SE analysis both supported the claims from the viscosity. The sedimentation coefficient was shown to be ~1.4 S, indicative of a small molecule. In addition the SE analysis showed that the molecular weight of the β-glucans was ~10kDa. The low molecular weight is supportive of literature values, however not possible as low as this. Using the [η], *s* and an array of hydration values, the shape of the β-glucans were determined to be extended prolates in all models.

With regard to the oat β-glucans the intrinsic viscosities were shown to be much larger, ranging from 400-1000 mL/g on average. This is immensely larger than the intrinsic viscosities of the mushroom β-glucans, however literature values suggest that oat β-glucans give rise to viscous solutions. The sedimentation coefficients obtained are also consistent with values previously found (Woodward et al., 1983). Comparisons of the apparent weight average molecular masses (at 1.5 mg/mL) show that all 6 oat β-glucans have very high molecular weights.

6.3.1 Future work

Once the full concentration extrapolations of the apparent weight average molecular weights to zero concentration (to eliminate the effects of non-ideality) have been performed on the 6 oat β-glucans, full conformation analysis using Mark-Houwink analysis can be performed. It will be intriguing to see if these molecules conform to a rigid conformation - as for the very short mushroom β,1-3, β,1-6 glucans, or (as is more likely) are more flexible structures, as seen for other larger β, 1-3, β,1-4 glucans from wheat (Li et al., 2006).

7 References

AN, H., PEAVY, T., HEDRICK, J. & LEBRILLA, C. (2003). Determination of N-Glycosylation Sites and Site Heterogeneity in Glycoproteins. Analytical Chemistry. 75 (20), p5628-5637.

BANSIL, R. & TURNER, B. (2006). Mucin structure, aggregation, physiological functions and biomedical applications. Current Opinion in Colloid & Interface Science. 11 (2-3), pp164-170.

BARNA, J. C. J., & WILLIAMS, D. H. (1984). The Structure and Mode of Action of Glycopeptide Antibiotics of the Vancomycin Group. Annual reviews of Microbiology. 38 (1), pp339-357.

BINDA, E., MARINELLI, F. & MARCONE, G. (2014). Old and New Glycopeptide Antibiotics: Action and Resistance. Antibiotics. 3 (4), pp572-594.

BRENNAN, C. & CLEARY, L. (2005). The potential use of cereal (1→3, 1→4)-β-d-glucans as functional food ingredients. *Journal of Cereal Science*. 42 (1), pp1-13.

BROWN, P. & SCHUCK, P. (2006). Macromolecular Size-and-Shape Distributions by Sedimentation Velocity Analytical Ultracentrifugation. *Biophysical Chemistry*. 90 (12), pp4651-4661.

BURTON, R., GIDLEY, M. & FINCHER, G. (2010). Heterogeneity in the chemistry, structure and function of plant cell walls. *Nature Chemical Biology*. 6 (10), pp724-732.

CARRELL, R. & OWEN, M. (1985). Plakalbumin, α1-antitrypsin, antithrombin and the mechanism of inflammatory thrombosis Plakalbumin, α1-antitrypsin, antithrombin and the mechanism of inflammatory thrombosis. *Nature*. 317 (6039), pp730-732.

CATALDO, M.A., TACCONELLI, E., GRILLI, E., PEA, F. & PETROSILLO, N. (2012). Continuous versus intermittent infusion of vancomycin for the treatment of Gram-positive infections: systematic review and meta-analysis. Journal of Antimicrobial Chemotherapy. 67 (1), pp17-24.

COLE, J., LARY, J., MOODY, T. & LAUE, T. (2008). Analytical Ultracentrifugation: Sedimentation Velocity and Sedimentation Equilibrium. *Methods in Cell Biology*. 84 (1), pp143-179.

CREETH, J.M. & HARDING, S.E. (1982). Some observations on a new type of point average molecular weight. *Journal of Biochemical and Biophysical Methods*. 7 (1), pp25-34.

CUI, W., WOOD, P.J., BLACKWELL, B. & NIKIFORUK, J. (2000). Physicochemical properties and structural characterization by two-dimensional NMR spectroscopy of wheat β-D-glucan—comparison with other cereal β-D-glucans. *Carbohydrate Polymers*. 41 (3), pp249-258.

DAOU, C. & ZHANG, H. (2012). Oat Beta-Glucan: It's Role in Health Promotion and Prevention of Diseases. *Comprehensive Reviews in Food Science and Food Safety*. 11 (4), pp355-365.

DE LA TORRE, J.G. & HARDING, S.E. (2013). Hydrodynamic modelling of protein conformation in solution: ELLIPS and HYDRO. *Biophysical Reviews*. 5 (2), pp195-206.

DEACON, M., MCGURK, S., ROBERTS, C., WILLIAMS, P., TENDLER, S., DAVIES, M., DAVIS, S. & HARDING, S. E. (2000). Atomic force microscopy of gastric mucin and chitosan mucoadhesive systems. Biochemical Journal. 348 (3), pp557-563.

DOUBLIER, JP. & WOOD, P. (1995). Rheological Properties of Aqueous Solutions of (1 -3) (1-4)-β-D-Glucan from Oats (Avena sativa L.). *Cereal Chemistry*. 72 (4), pp335-340.

DURCHSCHLAG, H. & ZIPPER, P. (1994). Calculation of the partial volume of organic compounds and polymers. Progress in Colloid & Polymer Science. 94 (1), pp20-39.

FEKETY, R., SILVA, J., KAUFFMAN, C., BUGGY, B. & GUNNER-DEERY, H. (1989). Treatment of antibiotic-associated Clostridium difficile colitis with oral vancomycin: Comparison of two dosage regimens. *The American Journal of Medicine*. 86 (1), pp15-19.

GAMEL, T., ABDEL-AAL, E-S., AMES, N., DUSS, R. & TOSH, S. (2014). Enzymatic extraction of beta-glucan from oat bran cereals and oat crackers and optimisation of viscosity measurement. *Journal of Cereal Science*. 59 (1), pp33-40.

GARDETE, S. & TOMASZ, A. (2012). Mechanisms of vancomycin resistance in Staphylococcus aureus. *The Journal of Clinical Investigation*. 124 (7), pp2836-2840.

GILLIS, R.B., ADAMS, G.G., WOLF, B., BERRY, M., BESONG, T., CORFIELD, A., KOK, S., SIDEBOTTOM, R., LAFOND, D., ROWE, A.J. & HARDING, S.E. (2013). Molecular weight distribution analysis by ultracentrifugation: Adaptation of a new approach for mucins. *Carbohydrate Polymers*. 93 (1), pp178-183.

GOMEZ, C., NAVARRO, A., MANZANAREA, P., HORTA, A. & CARBONELL, J.V`. (1997). Physical and structural properties of barley (1 → 3), (1 → 4)-β-d-glucan. Part II. Viscosity, chain stiffness and macromolecular dimensions. *Carbohydrate Polymers*. 32 (1), pp17-22.

HAN, M., HAN, Y., HYUN, S. & SHIN, H. (2008). Solubilization of water-insoluble beta-glucan isolated from Ganoderma lucidum. *Journal of Environmental Biology*. 29 (2), pp237-242.

HARDING, S.E. (1981). Could egg albumin be egg shaped? *International Journal of Biological Macromolecules*. 3 (12), pp398-399.

HARDING, S. E. (1995). On the hydrodynamic analysis of macromolecular conformation. *Biophysical Chemistry*. 55 (1), pp69-93.

HARDING, S.E. (1997). The intrinsic viscosity of biological macromolecules. Progress in measurement, interpretation and application to structure in dilute solution. *Progress in Biophysics and Molecular Biology*. 68 (2-3), pp207-262.

Harding, S. E., HORTON, J. & COLFEN, H. (1997b). The ELLIPS suite of macromolecular conformation algorithms. *European Biophysics Journal*. 25 (1), pp347-359.

HARDING, S.E., DAVIS, S.S., DEACON, M.P. & FIEBRIG, I. (1999). Biopolymer mucoadhesives. Biotechnology & Genetic Engineering Review. 16 (1), pp41-86.

HARDING, S.E., SCHUCK, P., ABDELHAMEDD, A.S., ADAMS, G.G., KOK, M.S. & MORRIS, G.A. (2011). Extended Fujita approach to the molecular weight distribution of polysaccharides and other polymeric systems. *Methods*. 54 (1), pp136-144.

HARDING, S.E., TOMBS, M., ADAMS, G.G., PAULSEN, B., INNGJERDINGEN, K.T., BARSETT, H. (2017). *An Introduction to Polysaccharide Biotechnology*. 2nd ed. London: CRC Press Taylor & Francis Group. Pp2-3.

HARVEY, D., WING, D., KUSTER, B. & WILSON, I. (2000). Composition of N-linked carbohydrates from ovalbumin and co-purified glycoproteins. Journal of American Society for Mass Spectrometry. 11 (6), pp564-571.

HARDING, S.E, COLFEN, H. & AZIZ, Z. (2005). The ELLIPS Suite of Whole-Body Protein Conformation Algorithms for Microsoft WINDOWS. In: Scott, D.J., Harding, S. E. & Rowe, A.J *Analytical Ultracentrifugation: Techniques and Methods*. Cambridge: Royal Society of Chemistry. pp460-483.

HIRAMATSU, K. (2001). Vancomycin-resistant Staphylococcus aureus: a new model of antibiotic resistance. *The Lancet: Infectious Diseases*. 1 (3), pp147-155.

HO, H., SIEVENPIPER, J., ZURBAU, A., MEJIA, S., JOVANOVSKI, E., AU-YEUNG, F., JENKINS, A. & VUKSAN, V. (2016). The effect of oat β-glucan on LDL-cholesterol, non-HDL-cholesterol and apoB for CVD risk reduction: a systematic review and meta-analysis of randomised-controlled trials. *British Journal of Nutrition*. 116 (8), pp1369-1382.

HOJO, H. & NAKAHARA, Y. (2007). Recent Progress in the Field of Glycopeptide Synthesis. *Biopolymers*. 88 (2), pp308-324.

HUBNER, F., O'NEIL, T., CASHMAN, K. & ARENDT, E. (2010). The influence of germination conditions on beta-glucan, dietary fibre and phytate during the germination of oats and barley. *European Food Research and Technology*. 231 (1), pp27-35.

HUNTER, M. (1966). A Method for the Determination of Protein Partial Specific Volumes 1. *Journal of Physical Chemistry*. 70 (10), pp3285-3292.

HUNTINGDON, J. & STEIN, P. (2001). Structure and properties of ovalbumin. Journal of Chromatography B: Biomedical Sciences and Applications. 756 (1-2), p189-198.

IANESELLI, L., ZHANG, F., SKODA, M., JACOBS, R., MARTIN, R., CALLOW, S., PREVOST, S. & SCHREIBER, F. (2010). Protein-Protein Interactions in Ovalbumin Solutions Studied by Small-Angle Scattering: Effect of Ionic Strength and the Chemical Nature of Cations. *Journal of Physical Chemistry*. 114 (11), pp3776-3783.

JIA, Z., O'MARA, M., ZUEGGE, J., COOPER, M. & MARK, A. (2013). Vancomycin: ligand recognition, dimerization and super-complex formation. *FEBS Journal*. 280 (5), pp1294-1307.

JOHNSON, J. & YALKOWSKY, S. (2006). Reformulation of a new vancomycin analog: an example of the importance of buffer species and strength. American Association of Pharmaceutical Scientists. 7 (1), ppE1-E5.

JUMEL, K. (1994). PhD Dissertation. University of Nottingham, UK.

JUMEL, K., FIEBRIG, I. & HARDING, S.E. (1996). Rapid size distribution and purity analysis of gastric mucus glycoproteins by size exclusion chromatography/multi angle laser light scattering. *International Journal of Biological Macromolecules*. 18 (1-2), pp133-139.

KARARLI, T.T (1995). Comparison of the gastrointestinal anatomy, physiology, and biochemistry of humans and commonly used laboratory animals. *Biopharmaceutics & Drug Disposition*. 16 (5), pp351-380.

KIELY, M., MCKNIGHT, G. & SCHIMKE, R. (1976). Studies on the Attachment of Carbohydrate to Ovalbumin Nascent Chains in Hen Oviduct. *The Journal of Biological Chemistry*. 251 (18), pp5490-5495.

KIEMLE, S., ZHANG, X., ESKER, A., TORIZ, G., GATENHOLM, P. & COSGROVE, D. (2014). Role of (1,3)(1,4)-β-Glucan in Cell Walls: Interaction with Cellulose. *Biomacromolecules*. 15 (5), pp1727-1736.

KIM, H., DEONIER, R. & WILLIAMS, J.W. (1977). The investigation of self-association. *Chemical Reviews*. 77 (5), pp659-690.

KIMURA, Y., SUMIYOSHI, M., SUZUKI, T. & SAKANAKA, M. (2006). Antitumor and Antimetastatic Activity of a Novel Water-soluble Low Molecular Weight β-1, 3-D-Glucan (branch β-1,6) Isolated from Aureobasidium pullulans 1A1 Strain Black Yeast. *Anticancer Research*. 26 (6B), pp4131-4141.

KOSEKI, T., FUKUDA, T., KITABATAKE, N., DOI, E. (1989). Charaterisation of linear polymers induced by thermal denatruation of ovalbumin. *Food Hydrocolloids*. 3 (2), pp135-148.

KRATKY, O., LEOPALD, H. & STABINGER, H. (1973). The determination of the partial specific volume of proteins by the mechanical oscillator technique. *Methods in Enzymology*. 27 (1), 98-110.

LAMM. O. (1929). The differential equation of ultracentrifugation. *Zeitschrift für Physikalische Chemie (Journal of Physical Chemistry)*. 143 (2), pp177-190.

LAROCHE, C. & MICHAUD, P. (2007). New developments and prospective applications for bet (1,3) glucans. Recent Patents on Biotechnology. 1 (1), pp59-73.

LAZARIDOU, A., BILIADERIS, C. & IZYDORCZYK, M. (2003). Molecular size effects the rheological properties of oat β-glucans in solution and gels. *Food Hydrocolloids*. 17 (2), pp693-712.

LI, W., CUI, S. & KAKUDA, Y. (2006). Extraction, fractionation, structural and physical characterization of wheat β-d-glucans. *Carbohydrate Polymers*. 63 (3), pp408-416.

LINSDELL, H., TOIRON, C., BRUIX, M., RIVAS, G. & MENENDEZ, M. (1996). Dimerization of A82846B, vancomycin and ristocetin: influence on antibiotic complexation with cell wall model peptides. *Journal of Antibiotics*. 49 (2), pp181-193.

LOLL, P., MILLER, R., WEEKS, C. & AXELSEN, P. (1998). A ligand-mediated dimerisation mode of vancomycin. Chemistry & Biology. 5 (5), pp293-298.

LUCAS, R.A., BOWTLE, W.J. & RYDEN, R. (1987). Disposition of vancomycin in healthy volunteers from oral solution and semi-solid matrix capsules. *Journal of Clinical Pharmacy and Therapeutics*. 12 (1), pp27-31.

MINE, Y. (1995). Recent advances in the understanding of egg white protein functionality. Trends in Food Science & Technology. 6 (7), p225-232.

NEUBERG, A. (1938). Carbohydrates in protein I: The carbohydrate component of crystalline egg albumin. *Biochemical Journal*. 32 (9), p1435-1451.

NIETO, M. & PERKINS, H.R. (1971a). The specificity of combination between ristocetins and peptides related to bacterial cell-wall mucopeptide precursors. The Biochemical Journal. 124 (5), pp845-852.

NIETO, M. & PERKINS, H.R. (1971b). Physiochemical properties of vancomycin and iodovancomycin and their complexes with diacetyl-L-lysyl-D0alanyl-D-alanine. The Biochemical Journal. 123 (5), pp773-787.

NISBET, A., SAUNDRY, R., MOIR, A., FOTHERGILL, L. & FOTHERGILL, J. (1981). The Complete Amino-Acid Sequence of Hen Ovalbumin. European Journal of Biochemistry. 115 (2), p335-345.

ORTEGA, A. & GARCIA, DE LA TORRE. (2007). Equivalent radii and ratios of radii from solution properties as indicators of macromolecular conformation, shape and flexibility. *Biomacromolecules*. 8 (8), pp2464-2475.

PILLAI, R., REDMOND, M. & RODING, J. (2005). Anti-Wrinkle Therapy: Significant New Findings in the Non-Invasive Cosmetic Treatment of Skin Wrinkles with Beta-Glucan. International Journal of Cosmetic Science. 27 (5), pp292-297.

POGGIO, C., CECI, M., BELTRAMI, R., COLOMBO, M. & DAGNA, A. (2015). Viscosity of endodontic irrigants: Influence of temperature. *Dental Research Journal*. 12 (5), pp425-430.

POLSON, A. (1967). Variation and sedimentation coefficient with rotor velocity. *Biochemical Journal*. 104 (2), pp410-415.

RAHAR, S., SWAMI, G., NAGPAL, N., NAGPAL, M. & SINGH, G. (2011). Preparation, characterization, and biological properties of β-glucan. *Journal of Advanced Pharmaceutical Technology & Research*. 2 (2), pp94-103.

RALSTON, R. (1993). Introduction to analytical ultracentrifugation, Fullerton, Beckman Instruments.

RAMAKRISHNAN, B., BOEGGEMAN, E. & QASBA, P. (2012). Binding of N-Acetylglucosamine (GlcNAc) β1–6-branched Oligosaccharide Acceptors to β4-Galactosyltransferase I Reveals a New Ligand Binding Mode. *The Journal of Biological Chemistry*. 287 (34), pp28666-28674.

REYNOLDS, P.E. (1989). Structure, Biochemistry and mechanism of Action of Glycopeptide Antibiotics. European Journal of Clinical Microbiology and Infectious Diseases. 8 (11), pp943-950.

RHEE, S., CHO, S., KIM, K., CHA, D.S. & PARK, H.J. (2008). A comparative study of analytical methods for alkali-soluble β-glucan in medicinal mushroom, Chaga (Inonotus obliquus). *LWT Food Science and Technology*. 41 (3), pp545-549.

ROARK, D. E. & YPHANTIS, D. A. (1696). Studies of self-associating systems by equilibrium ultracentrifugation. *Annals of the New York Academy of Sciences*. 164 (1), pp245-278.

ROUBROEKS, J.P., MASTROMAURO, D.I., ANDERSSON, R., CHRISTENSEN, B.E. & AMAN, P. (2000). Molecular weight, structure, and shape of oat (1->3), (1->4)-beta-D-glucan fractions obtained by enzymatic degradation with lichenase. *Biomacromolecules*. 1 (4), pp584-591.

RYBAK, M., LOMAESTRO, B., ROTSCHAFER, J., MOELLERING, R., CRAIG, W., BILLETER, M., DALOVISIO, J. & LEVINE, D. (2009). Therapeutic monitoring of vancomycin in adult patients: A consensus review of the American Society of Health-System Pharmacists, and the Infectious Diseases Society of America. American Journal of Health-System Pharmacy. 66 (1), pp82-98.

SAKAI, T. (1968). Extrapolation procedures for intrinsic viscosity and for Huggins constant k. *Journal of Polymer Physics*. 6 (9), pp1659-1672.

SARI, M., PRANGE, A., LELLEY, J. & HAMBITZER, R. (2017). Screening of beta-glucan contents in commercially cultivated and wild growing mushrooms. Food Chemistry. 216 (2), pp45-51.

SCHUCK, P. & DEMELER, B. (1999). Direct Sedimentation Analysis of Interference Optical Data in Analytical Ultracentrifugation. *Biophysical Journal*. 76 (4), pp2288-2296.

SCHUCK, P. (2000). Size-Distribution Analysis of Macromolecules by Sedimentation Velocity Ultracentrifugation and Lamm Equation Modeling. *Biophysical Journal*. 78 (3), pp1606-1619.

SCHUCK, P., GILLIS, R., BESONG, T., ALMUTAIRI, F., ADAMS, G.G., ROWE, A. & HARDING, S.E. (2014). SEDFIT–MSTAR: molecular weight and molecular weight distribution analysis of polymers by sedimentation equilibrium in the ultracentrifuge. *Analyst*. 139 (1), pp79-92.

SMALL, P. & CHAMBERS, H. (1990). Vancomycin for Staphylococcus aureus endocarditis in intravenous drug users. *Antimicrobial Agents and Chemotherapy*. 34 (6), pp1227-1231.

SPIRO, R. (2002). Protein glycosylation: nature, distribution, enzymatic function and disease implications of glycopeptide bonds. *Glycobiology*. 12 (4), pp43-56.

STAHMANN, P., MONCHAU, N., SAHM, A., GAWRONSKI, M., CONRAD, H., SPINGER, T. & KOPP, F. (1995). Structural properties of native and sonicated cinerean, a β-(1 → 3) (1→6)-D-glucan produced by Botrytis cinerea. *Carbohydrate Research*. 266 (1), pp115-128.

SURAWICZ, C., BRANDT, L., BINION, D., ANANTHAKRISHNAN, A. & CURRY, S.R. (2013). Guidelines for Diagnosis, Treatment, and Prevention of Clostridium difficile Infections. *The American Journal of Gastroenterology*. 108 (4), pp478-498.

SVEDBERG, T. & FAHRAEUS, R. (1926). A new method for the determination of the molecular weight of the proteins. *Journal of the American Chemical Society*. 48 (2), pp430-438.

TAI, T., YAMASHITA, K., ITO, S. & KOBATA, A. (1977). Structures of the Carbohydrate Moiety of Ovalbumin Glycopeptide III and the Difference in Specificity of Endo-β-N-acetylglucosaminidases C_{II} and H*. *The Journal of Biological Chemistry*. 252 (19), p6687-6694.

TANFORD, C. (1961). Viscosity. In: TANFORD, C *Physical Chemistry of macromolecules*. New York: John Wiley & Sons. PP391-412.

VAN HAL, S.J., PATERSON, D.L. & LODISE, T.P. (2013). Systematic review and meta-analysis of vancomycin-induced nephrotoxicity associated with dosing schedules that maintain troughs between 15 and 20 milligrams per litre. *Antimicrobial Agents and Chemotherapy*. 57 (2), pp734-744.

VAN HOLDE, K.E. & BALDWIN, R.L. (1958). Rapid Attainment of Sedimentation Equilibrium. *The Journal of Physical Chemistry*. 62 (6), pp734-743.

VARUM, K., MARTINSEN, A. & SMIDSROD, O. (1991). Fractionation and viscometric characterization of a (1→3), (1→4)-β-d-glucan from oat, and universal calibration of a high-performance size-exclusion chromatographic system by the use of fractionated β. *Food Hydrocolloids*. 5 (4), pp363-374.

WANG, J.C., HU, S.H., LIANG, Z.C. & YEH, C.J. (2005). Optimization for the production of water-soluble polysaccharide from Pleurotus citrinopilateus in submerged culture and its antitumor effect. *Applied Microbiology and Biotechnology*. 67 (6), pp759-766.

WASSER, S.P. (2002). Medicinal mushrooms as a source of antitumor and immunomodulating polysaccharides. *Applied Microbiology and Biotechnology*. 60 (3), pp258-274.

WASSER, S.P. (2011). Current findings, future trends and unresolved problems in studies of medicinal mushrooms. *Applied Microbiology and Biotechnology*. 89 (5), pp1323-1232.

WILLIAMS, D. & BARDSLEY, B. (1999). The Vancomycin Group of Antibiotics and the Fight against Resistant Bacteria. Angewandte Chemie. 38 (9), pp1172-1193.

WOODWARD, J.R., PHILLIPS, D.R. & FINCHER, G.B. (1983). Water-soluble (1→3), (1→4)-β-d-glucans from barley (Hordeum vulgare) endosperm. Physicochemical properties. *Carbohydrate Polymers*. 3 (2), pp143-156.

YIM, G., THAKER, M., KOTEVA, K. 7 WRIGHT, G. (2014). Glycopeptide antibiotic biosynthesis. The Journal of Antibiotics. 67 (11), pp31-41.

ZHANG, M., ZHANG, L. & CHEUNG, P.C. (2003). Molecular Mass and Chain Conformation of Carboxymethylated Derivatives of β-Glucan from Sclerotia of Pleurotus tuber-regium. *Biopolymers*. 68 (2), pp150-159.

ZHU, F., DU, B., BIAN, Z. & XU, B. (2015). Beta-glucans from edible and medicinal mushrooms: Characteristics, physicochemical and biological activities. Journal of Food Composition and Analysis. 41 (8), pp165-173.